

On using the coating of different materials to reduce the cross
polarized scattering from a PEMC cylinder buried below a
rough surface



By
Muhammad Akhtar

SUBMITTED IN PARTIAL FULFILLMENT OF THE
REQUIREMENTS FOR THE DEGREE OF
DOCTOR OF PHILOSOPHY
AT
QUAID-I-AZAM UNIVERSITY
ISLAMABAD, PAKISTAN



QUAID-I-AZAM UNIVERSITY
Department of Electronics

Author's Declaration

I, Muhammad Akhtar hereby state that my PhD thesis titled
"On using the coating of different materials to reduce cross
polarized scattering from a PEMC cylinder buried below a rough
interface." is my own work and has not been submitted previously
by me for taking degree from Department of Electronics, Quaid-
i-Azam University Or anywhere else in the country/world.

At any time if my statement is found to be incorrect even after my
graduation, the university has the right to withdraw my PhD
degree.

Muhammad Akhtar

Date: _____



QUAID-I-AZAM UNIVERSITY
Department of Electronics

Plagiarism Undertaking

I solemnly declare that research work presented in the thesis titled

"On using the coating of different materials to reduce cross polarized scattering from a PEMC cylinder buried below a rough interface."

is solely my research work with no significant contribution from any other person. Small contribution/help wherever taken has been duly acknowledged and that complete thesis has been written by me.

I understand the zero tolerance policy of the HEC and Quaid-i-Azam University towards plagiarism. Therefore, I as an Author of the above titled thesis, declare that no portion of my thesis has been plagiarized and any material used as reference is properly referred/cited.

I undertake that if I am found guilty of any formal plagiarism in the above titled thesis even after award of PhD degree, the University reserves the rights to withdraw/revoke my PhD degree and that HEC and the University has the right to publish my name on the HEC/University Website on which names of students are placed who submitted plagiarized thesis.

Student/Author Signature: _____

Name: **Muhammad Akhtar**

Quaid-i-Azam University
Department of Electronics,

It is certified that the work contained in the dissertation titled "On using the coating of different materials to reduce the cross polarized scattering from a PEMC cylinder buried below a rough surface" is carried out and completed by Muhammad Akhtar under my supervision at Quaid-i-Azam University Islamabad, Pakistan.



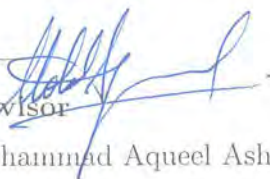
Advisor

Dr. Muhammad Arshad Fiaz

Assistant Professor

Department of Electronics

Quaid-i-Azam University Islamabad, Pakistan



Co-Advisor


Dr. Muhammad Aqueel Ashraf

Associate Professor

Department of Electronics

Quaid-i-Azam University Islamabad, Pakistan

Submitted through



Chairman

Prof. Dr. Syed Aqeel Abbas Bukhari

Department of Electronics

Quaid-i-Azam University Islamabad, Pakistan



QUAID-I-AZAM UNIVERSITY
Department of Electronics

Certificate of Approval


This is to certify that the research work presented in this thesis, entitled "**On using the coating of different materials to reduce cross polarized scattering from a PEMC cylinder buried below a rough interface.**" was conducted by **Mr. Muhammad Akhtar** under the supervision of **Dr. Muhammad Arshad Fiaz** and under the co-supervision of **Dr. Muhammad Aqueel Ashraf**. No part of this thesis has been submitted anywhere else for any other degree. This thesis is submitted to the **Department of Electronics, Quaid-i-Azam University** in partial fulfilment of the requirements for the degree of Doctor of Philosophy in Field of **Electronics**, Department of Electronics, Quaid-i-Azam University.

Student Name: **Mr. Muhammad Akhtar**


Signature: 

Examination Committee:

A. Dr. Hamid Saleem
Director General
National Center for Physics,
Shahdra Valley Road, Islamabad.

Signature: 

B. Prof, Dr. Manzoor Ikram
Professor
Center for Quantum Physics, COMSATS,
Pakistan Academy of Science Building,
G-5/2, Islamabad.

Signature: 

C. Dr. Muhammad Arshad Fiaz
Assistant Professor & Supervisor
Department of Electronics
Quaid-i-Azam University, Islamabad.

Signature: 

D. Dr. Muhammad Aqueel Ashraf
Associate Professor & Co-Supervisor
Department of Electronics
Quaid-i-Azam University, Islamabad.

Signature: _____

Supervisor Name: **Dr. Muhammad Arshad Fiaz**

Signature: 

Co-Supervisor Name: **Dr. Muhammad Aqueel Ashraf**

Signature: 

Name of Chairman: **Prof, Dr. Syed Aqeel A. Bukhari**

Signature: 

To my beloved family and respected teachers

Table of Contents

Table of Contents	vi
Acknowledgements	vii
List of publications included in the thesis	viii
1 Introduction	1
2 Theoretical analysis for scattering from a coated PEMC cylinder	6
2.1 Formulation for PEMC cylindrical core coated with CCM	6
2.2 Formulation for PEMC cylindrical core coated with chiral material . .	9
2.3 Formulation for PEMC cylindrical core coated with plasma material .	12
2.4 Formulation for PEMC cylindrical core coated with TI material . . .	13
3 Scattering from a PEMC cylindrical core coated with different materials and buried below a rough surface	16
3.1 Theoretical Formulation	16
3.1.1 Scattering from rough interface	17
3.1.2 Scattering from coated cylinder	19
4 Numerical results and discussions	22
4.1 Results for coating of CCM	22
4.2 Results for coating of chiral material	34
4.3 Results for coating of plasma material	40
4.4 Results for coating of topological insulator material	46
4.4.1 Comparison	52
References	57
Conclusion	57

Acknowledgements

With the grace of Almighty ALLAH who is the creator and guider of the universe. I would pay my acknowledgments to the Holy Prophet Mohammad (SAW), to whom this work is a humble dedication. I would like to thank those people who motivated and encouraged me to complete this work. I would like to thank my honorable and caring advisor Dr. M. Arshad Fiaz. Without his guidance and direction I was not able to complete this dissertation. I am thankful for consenting me precious suggestions. I could not have imagined having a better advisor for my Ph.D. other than Dr Muhammad Arshad Fiaz. I think this work would have not been possible without his kind supervision. I am also thankful to Dr. Muhammad Aqueel Ashraf for his guidance and cooperation throughout the studies.

I thank my friends Ashfaq Ahmad, Fahad Masood and other lab fellows for giving me company in this tenure. Moreover, I would like to thank my brother, sisters and every member of my family especially my wife for the continuous encouragement, prayers and support in my studies. Finally, I would like to dedicate this work to my parents, especially my father who motivated me at every stage of my studies.

Muhammad Akhtar

July, 2021

List of publications included in the thesis

1. M. Akhtar, M. A. Fiaz, and M. A. Ashraf, On using the complex conjugate material as coating to observe scattering from a PEMC cylinder buried below a sinusoidal slightly rough surface, *Optik*, Vol. 225: 165570, 2021.
2. M. Akhtar, M. A. Fiaz, M. A. Ashraf, Gaussian beam scattering from a DNG chiral coated PEMC cylinder buried below slightly rough surface, *Journal of Electromagnetic Waves and Applications*, Vol. 31, 912-926, 2017
3. M. Asghar, M. N. S. Qureshi, M. Akhtar, M. A. Fiaz, and M. A. Ashraf Scattering from anisotropic plasma-coated PEMC cylinder buried beneath a slightly rough surface, *Journal of Modern Optics*, Vol. 64, 2017) 101-110, 2017.

Abstract

Theoretical formulation is presented to evaluate the scattered fields from a perfect electromagnetic conductor (PEMC) cylindrical core coated with different materials and buried below a rough surface. Complex conjugate material (CCM), chiral material, plasma material and topological insulator (TI) material as coating are considered. To calculate the scattered field, perturbation theory (PT) and plane wave representation of fields are used. Far and near zone scattering patterns for the coating of different materials are observed. A comparison is presented with result obtained for the coating of dielectric material. For CCM coating, refractive index of the material is changed to note the change in scattering pattern while chirality is varied for the chiral coating. The effect of anisotropy is observed for the coating of plasma material while the cases of time reversal symmetry of TI material and symmetry broken are investigated by varying the value of magneto-electric parameter. Results are also reported by varying the thickness of the coating material, period of the surface, admittance of PEMC core. Finally a comparison is done between scattered fields for the coating of different materials as a function of thickness. It is observed that TI can be utilized for reducing cross polarized scattering while CCM is good for maximization of co polarized scattering. The amount of reduction depends on the polarization of the incident field, geometrical and physical parameters.

Chapter 1

Introduction

Scattering is the divergence of electromagnetic waves from their path due to an obstacle. The problem of scattering from objects embedded in another media has been undertaken by many researchers. The possible applications of such problems are detection of buried mines, localization of underground pipes and tunnels, determination of underground cracks and medical diagnosis. Moreover, it is required to simulate different scattering scenarios in view of ground penetrating radar to perform detection in different situations.

One of the simplest problem is scattering of electromagnetic waves from a perfect electric conductor (PEC) cylinder [1, 2]. The unknown is scattering amplitude (SA) which is determined by applying the boundary condition on the tangential components of the electric field at the surface of the cylinder. There is no transmitted field inside the PEC object. Multiple conducting cylinders are discussed in [3]. On the contrary, a dielectric cylinder has both scattered as well as transmitted fields. Scattering from a dielectric cylinder was studied in [4, 5]. Multiple dielectric cylinders are addressed in [6].

A circular cylinder made of complex conjugate material (CCM) was considered in [7]. In general, it is not possible to have non-attenuated light propagation when both the permittivity and permeability of a medium have complex values unless they are complex conjugate of each other. In this case, refractive index is real and the material is called complex conjugate material. Dragoman [8] explains how CCM can

be realized by arranging alternate layers of passive magnetic materials and active dielectrics/ semiconductor materials. Mathematically, it is defined by $\epsilon = m\mu^*$. For $\epsilon = p - iq$ and $\mu = p + iq$, the refractive index of a CCM is $n = \sqrt{m(p^2 + q^2)}$. A comparison between the scattered fields for the CCM and dielectric coatings with same value of the refractive index is worth investigating.

In contrast to dielectric/PEC cylinder, a metamaterial [9] cylinder can produce cross polarized field. Thus, theoretical and computational solutions become more complicated. Scattering from a cylinder made of double negative (DNG) metamaterial proposed by Veselago [10] was studied in [11]-[12]. Shelby performed the experimental verification of a negative index of refraction [13].

Scattering from chiral objects placed in free space has been presented in [14]. Multiple chiral cylinders were discussed in [15]. The optical activity is the ability of a chiral media to rotate the polarization [16]. Moreover, a linearly polarized wave splits into two waves (left and right circularly polarized) inside the chiral material. The constitutive relations in terms of chiral admittance ξ are given by [16]:

$$\mathbf{D} = \epsilon \mathbf{E} - j\xi \mathbf{B} \quad (1.0.1)$$

$$\mathbf{H} = \frac{\mathbf{B}}{\mu} - j\xi \mathbf{E} \quad (1.0.2)$$

The wave numbers are defined as

$$k_{\pm} = k[\sqrt{1 + \xi_r^2} \pm \xi_r] \quad (1.0.3)$$

where $k = \omega\sqrt{\mu\epsilon}$ and $\xi_r = \sqrt{\mu/\epsilon} \xi$.

Cross polarized scattered field from a perfect electromagnetic conductor (PEMC) cylinder has been evaluated by Ruppini [17]. A PEMC material does generalize both PEC and PMC materials [18]. The realization of a planar/cylindrical PEMC boundary has been proposed by using different configurations in [19]-[22]. At PEMC interface, the boundary conditions are defined using admittance parameter M as

$$\hat{u}_n \times (\mathbf{H} + M\mathbf{E}) = 0 \quad (1.0.4)$$

$$\hat{u}_n \cdot (\mathbf{D} - M\mathbf{B}) = 0 \quad (1.0.5)$$

where \hat{u}_n denotes the unit vector normal to the boundary surface. For the limit $M \rightarrow \pm\infty$, they are reduced to

$$\hat{u}_n \times \mathbf{E} = 0 \quad , \quad \hat{u}_n \cdot \mathbf{B} = 0 \quad (\text{PEC}) \quad (1.0.6)$$

while $M = 0$ gives

$$\hat{u}_n \times \mathbf{H} = 0 \quad , \quad \hat{u}_n \cdot \mathbf{D} = 0 \quad (\text{PMC}) \quad (1.0.7)$$

A cylinder made of plasma material is studied in [23]-[24]. Plasma being the fourth state of matter represents highly ionized state of a gas with a quasi-neutral mixture of electrons, neutral particles and free ions. A vehicle may experience the communications blackout due to plasma sheath. A coating of plasma sheath can significantly enhance or reduce the scattering cross section of an object. Artificial plasmas has created an opportunity for the new trends [25]. Anisotropic plasma is characterized by permittivity in tensor form

$$[\epsilon] = \begin{bmatrix} \epsilon_2 & j\epsilon_3 & 0 \\ -j\epsilon_3 & \epsilon_2 & 0 \\ 0 & 0 & \epsilon_4 \end{bmatrix}$$

where ϵ_2 , ϵ_3 and ϵ_4 are defined in [26] and are functions of electron density, collision frequency, and the strength of external magnetic field.

Scattering from a topological insulators (TI) cylinder was discussed in [27]. TI is a kind of special material that cannot be simply classified as conductor, insulator or semiconductor. Topological insulators [28]- [29] are nontrivial quantum states of matter which are defined by using both the topological field theory [30] and the topological band theory [31]. Being a new quantum state of matter, TIs are very promising materials for many applications in spintronics and electromagnetics. The cross polarization is another feature. Topological insulator is one of these objects that has co polarized as well as cross polarized scattering component like PEMC, chiral object etc. The constitutive relations in terms of fine structure constant α and axion

parameter θ describing the magneto-electric polarizability are given by [32]

$$\mathbf{D} = \epsilon \mathbf{E} + \frac{\alpha\theta}{\pi} \mathbf{B} \quad (1.0.8)$$

$$\mathbf{H} = \frac{1}{\mu} \mathbf{B} - \frac{\alpha\theta}{\pi} \mathbf{E} \quad (1.0.9)$$

The values of $\theta = 0$ and $\theta = \pi$ correspond to dielectric and TI materials, respectively. The time-reversal symmetry (TRS) in TI can be broken by either applying a weak magnetic field or a very thin magnetic coating [33, 34].

Scattering from cylinder coated with metamaterial has recently been focused [35]-[37]. Li and Shen observed the scattering from a PEC cylinder coated with DNG metamaterial [35]. Irci [36] used the metamaterial coating to achieve transparency and maximize scattering. A coated PEMC elliptic cylinder was considered in [37] and a chiral coated PEMC cylinder was studied in [38]. Use of plasma material as coating is done in [39]-[42]. Thus, the coating of different materials can be utilized for RCS reduction/cloaking, RCS enhancement/focusing and to study the surface plasmon polaritons properties [43, 44].

In all the above analysis, the cylinder is exposed directly to incident field and the problem formulation is relatively simple. It becomes complicated when cylinder is buried below a dielectric interface and only the interface is directly illuminated by an incident wave. Scattering of waves from buried cylinders is one important class of problem in this category and observation of scattering is usually done above the interface. Using the eigenfunction expansion of a two-dimensional Fredholm integral equation, scattering from a subterranean inhomogeneity is solved by Howard [45]. The work done by D'Yakonov [46] for a current line source above a uniform half-space has been extended by Ogunade [47]. Multipole expansion for the scattered field has been used by Mahmoud *et al.* [48]. A Green function approach is proposed by Budko [49].

A cylindrical obstacle is considered in [50]-[51] while multiple conducting and dielectric cylinders are taken by Divico *et al.* [52]-[53]. A TI cylinder was studied in [54] and a PEMC cylinder was considered in [55]. This problem models the ground

as a flat interface which can be considered as a special case of the general problem when the object is buried under a rough interface [56]. Rough surface scattering was evaluated using the perturbation theory (PT) whereas the multiple interactions between cylinder and rough interface were calculated by utilizing the plane wave representation of field. The same problem was solved by using the cylindrical wave approach by Fiaz *et al.* [57]. Utilizing the first order perturbation theory (PT)[58]-[59] to deal with slightly rough surface scattering has an advantage that a flat interface is a special case. The PT is applicable when both the height and slope of the surface $f(x)$ are small, i.e., $|f(x)| \ll 1, |\partial f(x)/\partial x| \ll 1$. Moreover, Kirchhoff approximation is used for large radius of curvature [60]. The study was presented for a Gaussian rough surface in [61]-[63]. In [64], a DNG coated PEMC cylinder was assumed. Use of chiral coating is done in [65] to reduce radar cross section (RCS) of PEC cylinder while the coating of TI material is proposed in [66].

In this work, a PEMC cylinder coated with different materials and buried below a rough interface is considered. This may be considered a general problem investigating all the above cited scenarios. By choosing the thickness of the coating equal to zero, scattering from a non coated PEMC cylinder can be obtained. For large admittance M , PEC case can be obtained while PMC case is defined by $M = 0$. Materials such as CCM, chiral, plasma, and TI are used as coating on PEMC cylindrical core. Results are reported for both co and cross polarized scattering. An effort has been made to compare the results with dielectric coating. Also, results are compared for coating materials considered in this thesis. The purpose is to investigate the scenario in which cross polarized field can be reduced.

In chapter 2, scattering coefficients are calculated for a PEMC cylinder coated with CCM, chiral, plasma, and TI materials. Chapter 3 contains the discussion when the cylinder is buried below a rough surface whereas results are reported in chapter 4.

Chapter 2

Theoretical analysis for scattering from a coated PEMC cylinder

In this chapter, different materials are used as coating on the PEMC cylindrical core to study the scattering properties. By imposing the boundary conditions for each of the coating material, the unknown scattering coefficients are evaluated. In section 2.1, complex conjugate material (CCM) is used as coating while chiral material is utilized in section 2.2. Plasma material and topological insulator (TI) material are used for coating in sections 2.3 and 2.4 respectively. The time dependency is assumed $e^{j\omega t}$.

2.1 Formulation for PEMC cylindrical core coated with CCM

Consider a PEMC cylindrical core coated with CCM as shown in Figure 2.1. The radius/size of the core is a while that of the coated cylinder is b . A TM polarized incident field (electric field is parallel to cylinder axis) is given by

$$E_i^z = e^{-j(k_x^i x - k_{0y}^i y)}. \quad (2.1.1)$$

The incident magnetic field is written as

$$H_i^\phi = \frac{1}{j\eta_1} e^{-j(k_x^i x - k_{0y}^i y)} \quad (2.1.2)$$

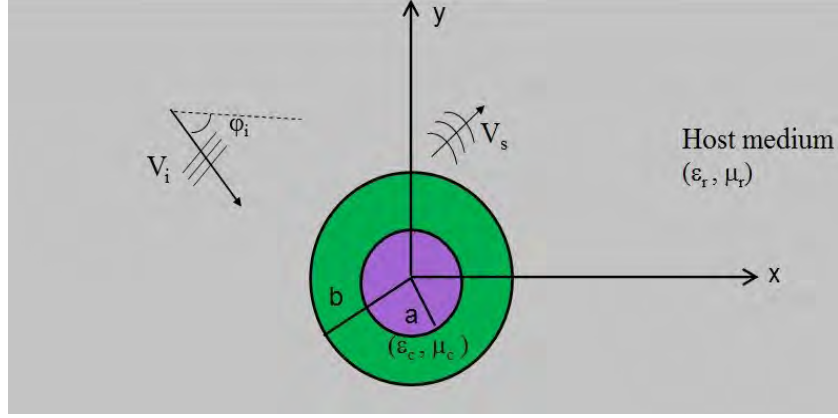


Figure 2.1: Scattering scenario: a coated PEMC circular cylinder.

In polar coordinates, the incident electric and magnetic fields can be defined in terms of Bessel function $J_n(\cdot)$ as

$$E_i^z = \sum_{n=-\infty}^{\infty} j^{-n} J_n(k_1 \rho) e^{jn(\varphi - \varphi_i)} \quad (2.1.3)$$

$$H_i^\phi = \frac{1}{j\eta_1} \sum_{n=-\infty}^{\infty} j^{-n} J'_n(k_1 \rho) e^{jn(\varphi - \varphi_i)} \quad (2.1.4)$$

where $\eta_1 = \sqrt{\mu_1/\epsilon_1}$ is the impedance of the host medium.

The scattered field can be represented with Hankel function $H_n^{(2)}(\cdot)$ as basis functions and unknown scattering coefficients A_n (co polarized) and B_n (cross polarized) as

$$E_s = \sum_{n=-\infty}^{\infty} j^{-n} \left[\hat{z} A_n H_n^{(2)}(k_1 \rho) + \hat{\phi} B_n H_n'^{(2)}(k_1 \rho) \right] e^{jn(\varphi - \varphi_i)} \quad (2.1.5)$$

$$H_s = \frac{1}{j\eta_1} \sum_{n=-\infty}^{\infty} j^{-n} \left[\hat{z} B_n H_n^{(2)}(k_1 \rho) + \hat{\phi} A_n H_n'^{(2)}(k_1 \rho) \right] e^{jn(\varphi - \varphi_i)} \quad (2.1.6)$$

The transmitted electric and magnetic fields into the coating material are given

by

$$E_c = \sum_{n=-\infty}^{\infty} j^{-n} \left[\hat{z}(C_n H_n^{(2)}(k_2 \rho) + D_n H_n^{(1)}(k_2 \rho)) + \hat{\phi}(E_n H_n'^{(2)}(k_2 \rho) + F_n H_n'^{(1)}(k_2 \rho)) \right] e^{jn(\varphi - \varphi_i)} \quad (2.1.7)$$

$$H_c = \frac{1}{j\eta} \sum_{n=-\infty}^{\infty} j^{-n} \left[\hat{\phi}(C_n H_n'^{(2)}(k_2 \rho) + D_n H_n'^{(1)}(k_2 \rho)) + \hat{z}(E_n H_n^{(2)}(k_2 \rho) + F_n H_n^{(1)}(k_2 \rho)) \right] e^{jn(\varphi - \varphi_i)} \quad (2.1.8)$$

where $\eta = \sqrt{\mu_c/\epsilon_c}$ is the impedance of the coating material. The unknowns can be found by the following boundary conditions

$$\begin{aligned} H_c^z + M E_c^z &= 0 & \rho &= a \\ H_c^\phi + M E_c^\phi &= 0 & \rho &= a \\ H_i^\phi + H_s^\phi &= H_c^\phi & \rho &= b \\ E_i^z + E_s^z &= E_c^z & \rho &= b \\ E_s^\phi &= E_c^\phi & \rho &= b \\ H_s^z &= H_c^z & \rho &= b \end{aligned} \quad (2.1.9)$$

Putting equations (2.1.3)-(2.1.8) into the above boundary conditions, we obtain the following system of equations [70]

$$\mathbf{W}\mathbf{X} = \mathbf{U} \quad (2.1.10)$$

where

$$\begin{aligned} \mathbf{X} &= \begin{bmatrix} A_n, B_n, C_n, D_n, E_n, F_n \end{bmatrix}^T \\ \mathbf{U} &= \begin{bmatrix} 0, 0, J_n(\beta_1), J_n'(\beta_1), 0, 0 \end{bmatrix}^T \\ \mathbf{W} &= \begin{bmatrix} 0 & 0 & c_4 H_n^{(2)}(\alpha_2) & c_4 H_n^{(1)}(\alpha_2) & H_n^{(2)}(\alpha_2) & H_n^{(1)}(\alpha_2) \\ 0 & 0 & H_n^{(2)'}(\alpha_2) & H_n^{(1)'}(\alpha_2) & c_4 H_n^{(2)'}(\alpha_2) & c_4 H_n^{(1)'}(\alpha_2) \\ -H_n^{(2)}(\beta_1) & 0 & H_n^{(2)}(\beta_2) & H_n^{(1)}(\beta_2) & 0 & 0 \\ -H_n^{(2)'}(\beta_1) & 0 & c_3 H_n^{(2)'}(\beta_2) & c_3 H_n^{(1)'}(\beta_2) & 0 & 0 \\ 0 & -H_n^{(2)}(\beta_1) & 0 & 0 & c_3 H_n^{(2)}(\beta_2) & c_3 H_n^{(1)}(\beta_2) \\ 0 & -H_n^{(2)'}(\beta_1) & 0 & 0 & H_n^{(2)'}(\beta_2) & H_n^{(1)'}(\beta_2) \end{bmatrix} \end{aligned}$$

being $\beta_1 = k_1 b$, $\beta_2 = k_2 b$, $\alpha_2 = k_2 a$ and

$$c_3 = \frac{\eta_1}{\eta} \quad \text{TM polarization} \quad (2.1.11)$$

$$c_4 = jM\eta \quad \text{TM polarization} \quad (2.1.12)$$

For TE polarized field (electric field is transverse to cylinder axis),

$$c_3 = \frac{\eta}{\eta_1} \quad \text{TE polarization} \quad (2.1.13)$$

$$c_4 = \frac{j}{M\eta} \quad \text{TE polarization} \quad (2.1.14)$$

By solving the above system of equations, the unknown scattering coefficients can be obtained for scattering from a PEMC cylinder coated with CCM material. The following scattering scenarios can also be simulated:

- A PEMC cylinder coated with dielectric material;
- A non coated PEMC cylinder by selecting $\epsilon_1 = \epsilon_c$;
- A PEMC cylinder coated with DNG material for $\epsilon_c < 0, \mu_c < 0$;
- A PEC cylinder coated with CCM/dielectric material as $M \rightarrow \infty$;
- A PMC cylinder coated with CCM/dielectric material when $M = 0$;

2.2 Formulation for PEMC cylindrical core coated with chiral material

Now, consider a PEMC core coated with chiral material. The incident fields are given by

$$E_i = \sum_{n=-\infty}^{\infty} j^{-n} J_n(k_1 \rho) e^{jn(\varphi - \varphi_i)} \quad (2.2.1)$$

$$H_i = \frac{1}{j\eta_1} \sum_{n=-\infty}^{\infty} j^{-n} J'_n(k_1 \rho) e^{jn(\varphi - \varphi_i)} \quad (2.2.2)$$

Scattered fields are given by

$$E_s = \sum_{n=-\infty}^{\infty} j^{-n} \left[\hat{z} A_n H_n^{(2)}(k_1 \rho) + \hat{\phi} B_n H_n^{(2)'}(k_1 \rho) \right] e^{jn(\varphi - \varphi_i)} \quad (2.2.3)$$

$$H_s = \frac{1}{j\eta_1} \sum_{n=-\infty}^{\infty} j^{-n} \left[\hat{z} B_n H_n^{(2)}(k_1 \rho) + \hat{\phi} A_n H_n^{(2)'}(k_1 \rho) \right] e^{jn(\varphi - \varphi_i)} \quad (2.2.4)$$

where A_n are co polarized scattering coefficients and B_n are cross polarized scattering coefficients.

Transmitted fields inside the coating are left and right circularly polarized waves and they are given by

$$\begin{aligned} E_c = & \sum_{n=-\infty}^{\infty} j^{-n} \left[\hat{z} \left(C_n J_n(k_+ \rho) - D_n J_n(k_- \rho) + E_n H_n^{(2)}(k_+ \rho) - F_n H_n^{(2)}(k_- \rho) \right) \right. \\ & \left. + \hat{\phi} \left(C_n J_n'(k_+ \rho) + D_n J_n'(k_- \rho) + E_n H_n'^{(2)}(k_+ \rho) + F_n H_n'^{(2)}(k_- \rho) \right) \right] e^{jn(\varphi - \varphi_i)} \end{aligned} \quad (2.2.5)$$

$$\begin{aligned} H_c = & \frac{1}{j\eta} \sum_{n=-\infty}^{\infty} j^{-n} \left[\hat{\phi} \left(C_n J_n'(k_+ \rho) + D_n J_n'(k_- \rho) + E_n H_n'^{(2)}(k_+ \rho) + F_n H_n'^{(2)}(k_- \rho) \right) \right. \\ & \left. + \hat{z} \left(C_n J_n(k_+ \rho) - D_n J_n(k_- \rho) + E_n H_n^{(2)}(k_+ \rho) - F_n H_n^{(2)}(k_- \rho) \right) \right] e^{jn(\varphi - \varphi_i)} \end{aligned} \quad (2.2.6)$$

where $\eta = \sqrt{\mu_0/[\epsilon(1 + x_c^2)]}$ and $x_c = \sqrt{\mu/\epsilon} \xi$ with ξ is the chiral admittance.

The boundary conditions can be written as

$$\begin{aligned} H_c^z + M E_c^z &= 0 & \rho = a \\ H_c^\phi + M E_c^\phi &= 0 & \rho = a \\ H_t^\phi + H_s^\phi &= H_c^\phi & \rho = b \\ E_t^z + E_s^z &= E_c^z & \rho = b \\ E_s^\phi &= E_c^\phi & \rho = b \\ H_s^z &= H_c^z & \rho = b \end{aligned} \quad (2.2.7)$$

Putting the expressions into equation (2.2.7), the unknowns can be obtained as [69]

$$\mathbf{W}\mathbf{X} = \mathbf{U} \quad (2.2.8)$$

where

$$\begin{aligned} \mathbf{X} &= \begin{bmatrix} A_n, B_n, C_n, D_n, E_n, F_n \end{bmatrix}^T \\ \mathbf{U} &= \begin{bmatrix} 0, 0, 0, 0, J_n(\beta_1), c_3 J'_n(\beta_1) \end{bmatrix}^T \\ \mathbf{W} &= \begin{bmatrix} 0 & 0 & c_1 J_n(\alpha_+) & -c_1 J_n(\alpha_-) & c_1 H_n^{(2)}(\alpha_+) & -c_1 H_n^{(2)}(\alpha_-) \\ 0 & 0 & c_1 J'_n(\alpha_+) & c_1 J'_n(\alpha_-) & c_1 H_n^{(2)'}(\alpha_+) & c_1 H_n^{(2)'}(\alpha_-) \\ 0 & -\eta_t H_n^{(2)}(k_1 b) & J_n(\beta_+) & J_n(\beta_-) & H_n^{(2)}(\beta_+) & H_n^{(2)}(\beta_-) \\ 0 & -H_n^{(2)'}(k_1 b) & J'_n(\beta_+) & J'_n(\beta_-) & H_n^{(2)'}(\beta_+) & H_n^{(2)'}(\beta_-) \\ -H_n^{(2)}(\beta_1) & 0 & J_n(\beta_+) & -J_n(\beta_-) & H_n^{(2)}(\beta_+) & -H_n^{(2)}(\beta_-) \\ -c_3 H_n^{(2)'}(\beta_1) & 0 & J'_n(\beta_+) & -J'_n(\beta_-) & H_n^{(2)'}(\beta_+) & -H_n^{(2)'}(\beta_-) \end{bmatrix} \end{aligned}$$

and $c_1 = (jM\eta + 1)$, $c_3 = \eta/\eta_1$, $\alpha_+ = k_+ a$, $\alpha_- = k_- a$, $\beta_+ = k_+ b$, $\beta_- = k_- b$. For TE polarization, $c_1 = (jM\eta - 1)$, $c_3 = \eta_1/\eta$.

The solution of the above system of equations gives the scattering from a PEMC cylinder coated with chiral material. The following special cases can also be derived to study scattering from a:

- Dielectric coated PEMC cylinder by selecting $\xi = 0$;
- DNG chiral coated PEMC cylinder when $\epsilon_c < 0, \mu_c < 0$;
- A PEC cylinder coated with chiral/dielectric material as $M \rightarrow \infty$;
- A PMC cylinder coated with chiral/dielectric material when $M = 0$;

2.3 Formulation for PEMC cylindrical core coated with plasma material

Now, consider a PEMC core coated with plasma material. The incident fields are

$$E_z^i = \sum_{n=-\infty}^{\infty} j^{-n} J_n(k_1 \rho) e^{jn(\varphi - \varphi_i)} \quad (2.3.1)$$

$$H_\phi^i = \frac{1}{j\eta_1} \sum_{n=-\infty}^{\infty} j^{-n} J'_n(k_1 \rho) e^{jn(\varphi - \varphi_i)} \quad (2.3.2)$$

The scattered field are

$$E^s = \sum_{n=-\infty}^{\infty} j^{-n} \left[\hat{z} A_n H_n^{(2)}(k_1 \rho) + \hat{\phi} B_n H_n^{(2)'}(k_1 \rho) \right] e^{jn(\varphi - \varphi_i)} \quad (2.3.3)$$

$$H^s = \frac{1}{j\eta_1} \sum_{n=-\infty}^{\infty} j^{-n} \left[\hat{z} B_n H_n^{(2)}(k_1 \rho) + \hat{\phi} A_n H_n^{(2)'}(k_1 \rho) \right] e^{jn(\varphi - \varphi_i)} \quad (2.3.4)$$

The transmitted fields inside the coating are

$$E_c = \sum_{n=-\infty}^{\infty} j^n \left[\hat{z} (C_n H_n^{(2)}(k_2 \rho) + D_n H_n^{(1)}(k_2 \rho)) + \hat{\phi} (E_n H_n^{(2)'}(k_3 \rho) + F_n H_n^{(1)'}(k_3 \rho)) \right] e^{jn(\varphi - \varphi_i)} \quad (2.3.5)$$

$$H_c = \frac{1}{j\eta} \sum_{n=-\infty}^{\infty} j^n \left[\hat{\phi} (C_n H_n^{(2)'}(k_2 \rho) + D_n H_n^{(1)'}(k_2 \rho)) + \hat{z} (E_n H_n^{(2)}(k_3 \rho) + F_n H_n^{(1)}(k_3 \rho)) \right] e^{jn(\phi - \phi_i)} \quad (2.3.6)$$

where $k_2 = k_0/\sqrt{m_1}$, $k_3 = k_0/\sqrt{m_4}$, $\eta_2 = \sqrt{m_1 \mu_2}$, $m_1 = \epsilon_2/(\epsilon_2^2 - \epsilon_3^2)$, and $m_4 = 1/\epsilon_4$.

The boundary conditions are given by

$$\begin{aligned} H_z^c + M E_z^c &= 0 & \rho &= a \\ H_\phi^c + M E_\phi^c &= 0 & \rho &= a \\ H_\phi^i + H_\phi^s &= H_\phi^c & \rho &= b \\ E_z^i + E_z^s &= E_z^c & \rho &= b \\ E_\phi^s &= E_\phi^c & \rho &= b \\ H_z^s &= H_z^c & \rho &= b \end{aligned} \quad (2.3.7)$$

The system of linear equations to find the unknowns is given as [68]

$$\mathbf{W}\mathbf{X} = \mathbf{U} \quad (2.3.8)$$

where

$$\begin{aligned} \mathbf{X} &= \begin{bmatrix} A_n, B_n, C_n, D_n, E_n, F_n \end{bmatrix}^T \\ \mathbf{U} &= \begin{bmatrix} 0, 0, J_n(\beta_1), J'_n(\beta_1), 0, 0 \end{bmatrix}^T \\ \mathbf{W} &= \begin{bmatrix} 0 & 0 & c_4 H_n^{(2)}(\alpha_2) & c_4 H_n^{(1)}(\alpha_2) & H_n^{(2)}(\alpha_3) & H_n^{(1)}(\alpha_3) \\ 0 & 0 & H_n^{(2)'}(\alpha_2) & H_n^{(1)'}(\alpha_2) & c_4 H_n^{(2)'}(\alpha_3) & c_4 H_n^{(1)'}(\alpha_3) \\ -H_n^{(2)}(\beta_1) & 0 & H_n^{(2)}(\beta_2) & H_n^{(1)}(\beta_2) & 0 & 0 \\ -H_n^{(2)'}(\beta_1) & 0 & c_3 H_n^{(2)'}(\beta_2) & c_3 H_n^{(1)'}(\beta_2) & 0 & 0 \\ 0 & -H_n^{(2)}(\beta_1) & 0 & 0 & c_3 H_n^{(2)}(\beta_3) & c_3 H_n^{(1)}(\beta_3) \\ 0 & -H_n^{(2)'}(\beta_1) & 0 & 0 & H_n^{(2)'}(\beta_3) & H_n^{(1)'}(\beta_3) \end{bmatrix} \end{aligned}$$

where $c_3 = \eta_1/\eta$, $c_4 = jM\eta$, $\beta_1 = k_1b$, $\beta_2 = k_2b$, $\beta_3 = k_3b$, $\alpha_2 = k_2a$, and $\alpha_3 = k_3a$.

For TE polarization, $c_3 = \eta/\eta_1$, $c_4 = j/(M\eta)$.

By selecting the proper parameters, the following special cases are obtained

- A PEMC cylinder coated with isotropic plasma for $\epsilon_3 = 0, \epsilon_2 = \epsilon_4$;
- A non coated PEMC cylinder for $\epsilon_3 = 0, \epsilon_1 = \epsilon_2 = \epsilon_4$;
- A DNG coated PEMC cylinder for $\epsilon_3 = 0, \epsilon_2 = \epsilon_4 < 0, \mu_2 < 0$;
- A PEC coated cylinder when $M \rightarrow \infty$;
- A PMC coated cylinder when $M = 0$;

2.4 Formulation for PEMC cylindrical core coated with TI material

Now consider the TI material as coating. The incident fields are

$$E_i^z = \sum_{n=-\infty}^{\infty} j^{-n} J_n(k_1 \rho) e^{jn\phi} \quad (2.4.1)$$

$$H_i^\phi = \frac{1}{j\eta_1} \sum_{n=-\infty}^{\infty} j^{-n} J'_n(k_1\rho) e^{jn(\varphi-\varphi_i)} \quad (2.4.2)$$

The scattered fields are

$$\mathbf{E}_s = \sum_{n=-\infty}^{\infty} i^{-n} \left[\hat{z} A_n H_n^{(2)}(k_1\rho) + \hat{\phi} B_n H_n^{(2)'}(k_1\rho) \right] e^{jn(\varphi-\varphi_i)} \quad (2.4.3)$$

$$\mathbf{H}_s = \frac{1}{j\eta_1} \sum_{n=-\infty}^{\infty} i^{-n} \left[\hat{z} B_n H_n^{(2)}(k_1\rho) + \hat{\phi} A_n H_n^{(2)'}(k_1\rho) \right] e^{jn(\varphi-\varphi_i)} \quad (2.4.4)$$

Inside the coating material, the fields are given by

$$\begin{aligned} \mathbf{E}_c = & \sum_{n=-\infty}^{\infty} i^{-n} \left[\hat{z} \left(C_n H_n^{(2)}(k_2\rho) + D_n H_n^{(1)}(k_2\rho) \right) \right. \\ & \left. + \hat{\phi} \left(E_n H_n^{(2)'}(k_2\rho) + F_n H_n^{(1)'}(k_2\rho) \right) \right] e^{jn(\varphi-\varphi_i)} \end{aligned} \quad (2.4.5)$$

$$\begin{aligned} \mathbf{B}_c = & \mu \frac{1}{j\eta} \sum_{n=-\infty}^{\infty} i^{-n} \left[\hat{z} \left(E_n H_n^{(2)}(k_2\rho) + F_n H_n^{(1)}(k_2\rho) \right) \right. \\ & \left. + \hat{\phi} \left(C_n H_n^{(2)'}(k_2\rho) + D_n H_n^{(1)'}(k_2\rho) \right) \right] e^{jn(\varphi-\varphi_i)} \end{aligned} \quad (2.4.6)$$

Using the constitutive relation defined in equation (1.0.9), the boundary conditions are expressed as [66]

$$\begin{aligned} \frac{1}{\mu} B_c^z + (M - \alpha \frac{\theta}{\pi}) E_c^z &= 0 & \rho = a \\ \frac{1}{\mu} B_c^\phi + (M - \alpha \frac{\theta}{\pi}) E_c^\phi &= 0 & \rho = a \end{aligned} \quad (2.4.7)$$

$$\begin{aligned} H_s^z &= \frac{1}{\mu} B_c^z - \alpha \frac{\theta}{\pi} E_c^z & \rho = b \\ E_s^\phi &= E_c^\phi & \rho = b \\ E_t^z + E_s^z &= E_c^z & \rho = b \\ H_t^\phi + H_s^\phi &= \frac{1}{\mu} B_c^\phi - \alpha \frac{\theta}{\pi} E_c^\phi & \rho = b \end{aligned} \quad (2.4.8)$$

The following system of equations can be implemented to get the unknowns [66]

$$\mathbf{W}\mathbf{X} = \mathbf{U} \quad (2.4.9)$$

where

$$\begin{aligned}\mathbf{X} &= \begin{bmatrix} A_p, B_n, C_n, D_n, E_n, F_n \end{bmatrix}^T \\ \mathbf{U} &= \begin{bmatrix} 0, 0, 0, 0, J_n(\beta_1), J'_n(\beta_1) \end{bmatrix}^T \\ \mathbf{W} &= \begin{bmatrix} 0 & 0 & c_4 H_n^{(2)}(\alpha_2) & c_4 H_n^{(1)}(\alpha_2) & H_n^{(2)}(\alpha_2) & H_n^{(1)}(\alpha_2) \\ 0 & 0 & H_n^{(2)'}(\alpha_2) & H_n^{(1)'}(\alpha_2) & c_4 H_n^{(2)'}(\alpha_2) & c_4 H_n^{(1)'}(\alpha_2) \\ -H_n^{(2)}(\beta_1) & 0 & H_n^{(2)}(\beta_2) & H_n^{(1)}(\beta_2) & 0 & 0 \\ -H_n^{(2)'}(\beta_1) & 0 & c_3 H_n^{(2)'}(\beta_2) & c_3 H_n^{(1)'}(\beta_2) & 0 & 0 \\ 0 & -H_n^{(2)}(\beta_1) & c_5 H_n^{(2)}(\beta_2) & c_5 H_n^{(1)}(\beta_2) & c_3 H_n^{(2)}(\beta_2) & c_3 H_n^{(1)}(\beta_2) \\ 0 & -H_n^{(2)'}(\beta_1) & 0 & 0 & H_n^{(2)'}(\beta_2) & H_n^{(1)'}(\beta_2) \end{bmatrix}\end{aligned}$$

and $c_3 = (\eta_1/\eta)$, $c_4 = j\eta(M - \alpha\theta/\pi)$, $c_5 = -j\eta_1\alpha\theta/\pi$, $\beta_1 = k_1b$, $\alpha_2 = k_2a$, $\beta_2 = k_2b$. For TE polarization, $c_3 = \eta/\eta_1$, $c_4 = (j/\eta)(1/M - \alpha\theta/\pi)$, $c_5 = -(j/\eta_1)\alpha\theta/\pi$.

These problems can also be studied:

- A PEMC cylinder with dielectric coating ($\theta = 0$).
- A PEMC cylinder with coating of TRS ($\theta = \pi$) and TRS broken TI material ($\theta = 41\pi$);
- A PEC cylinder with coating of TI material when $M \rightarrow \infty$;
- A PMC cylinder with $M = 0$;

Chapter 3

Scattering from a PEMC cylindrical core coated with different materials and buried below a rough surface

In this chapter, scattering is presented from a PEMC cylindrical core coated with different materials and buried in a dielectric half space with rough surface. All the interactions between the rough surface and the buried object are evaluated in an iterative manner by writing the cylindrical waves into spectrum of plane waves. In section 3.1, problem formulation is discussed. Rough surface scattering is described in section 3.1.1 while multiple interactions are calculated in section 3.1.2.

3.1 Theoretical Formulation

Consider figure 3.1, a PEMC cylindrical core coated with different materials is buried in a dielectric half space with rough interface . The radius/size of the core is a while that of the coated cylinder is b . The depth of the buried object is d . The whole problem can be divided into two sub problems:

- Scattering from a rough interface.
- Scattering from a coated PEMC cylinder.

The interaction between the two scatterers is modeled by representing the cylindrical waves scattered by the cylinder into plane wave spectrum and calculating the reflection from the rough interface.

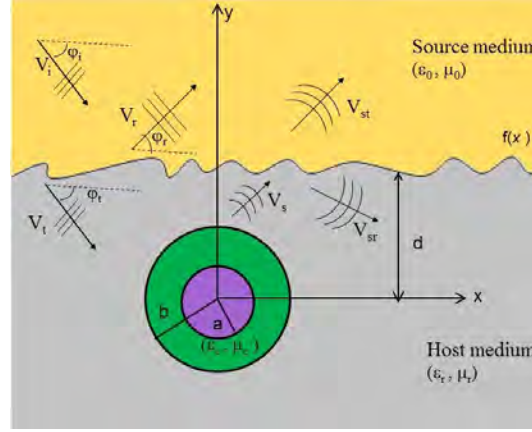


Figure 3.1: Scattering scenario: a PEMC cylindrical core coated with different materials and buried under a rough surface.

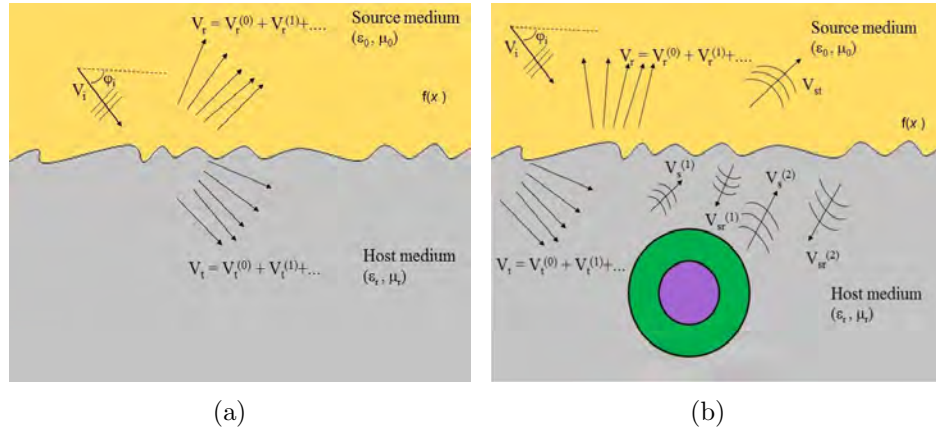


Figure 3.2: (a) Scattering from a rough interface using the PT. (b) Field components for the scattering scenario depicted in Figure 2.1.

3.1.1 Scattering from rough interface

Consider a rough surface $f(x)$ as shown in Figure 3.2(a). A plane wave is incident from the source medium on a rough surface at an angle φ_i . General expressions

representing the electric/magnetic field for TM/TE polarization are given.

The incident field is expressed as

$$V_i = e^{-j(k_x^i x - k_{0y}^i y)} \quad (3.1.1)$$

Using the first order perturbation method (PM), the field reflected from the rough surface can be expressed as

$$V_r = V_r^{(0)} + V_r^{(1)} + \dots \quad (3.1.2)$$

where $V_r^{(0)}$ is the reflected field due to flat interface and $V_r^{(1)}$ is the contribution by superimposed roughness, given as

$$V_r^{(0)} = \gamma_{01}^{(0)}(k_x^i) e^{j2k_{0y}^i d} e^{-j(k_x^i x + k_{0y}^i y)} \quad (3.1.3)$$

$$V_r^{(1)} = \int_{-\infty}^{\infty} \gamma_{01}^{(1)}(k_x) e^{j(k_{0y}^i + k_{0y})d} e^{-j(k_x x + k_{0y} y)} dk_x \quad (3.1.4)$$

The expressions for the unknown reflection coefficients are given in [56]. The transmitted field through rough surface can be expressed as

$$V_t = V_t^{(0)} + V_t^{(1)} + \dots \quad (3.1.5)$$

where

$$V_t^{(0)} = \tau_{01}^{(0)}(k_x^i) e^{j(k_{0y}^i - k_{1y}^i)d} e^{-j(k_x^i x - k_{1y}^i y)} \quad (3.1.6)$$

$$V_t^{(1)} = \int_{-\infty}^{\infty} \tau_{01}^{(1)}(k_x) e^{j(k_{0y}^i - k_{1y})d} e^{-j(k_x x - k_{1y} y)} dk_x \quad (3.1.7)$$

The transmission coefficients are given as [56],

$$\tau_{01}^{(0)TM}(k_x^i) = \frac{2k_{0y}^i}{k_{0y}^i + k_{1y}^i} \quad (3.1.8)$$

$$\tau_{01}^{(0)TE}(k_x^i) = \frac{2k_1^2 k_{0y}^i}{k_1^2 k_{0y}^i + k_0^2 k_{1y}^i} \quad (3.1.9)$$

$$\tau_{01}^{(1)TM}(k_x^i) = \frac{2k_{0y}^i(k_0^2 - k_1^2)}{(k_{0y}^i + k_{1y}^i)(k_{0y} + k_{1y})} jF(k_x - k_x^i) \quad (3.1.10)$$

$$\tau_{01}^{(1)TE}(k_x^i) = \frac{2k_1^2 k_{0y}^i(k_0^2 - k_1^2)(k_x^i k_x - k_{1y}^i k_{1y})}{(k_1^2 k_{0y}^i + k_0^2 k_{1y}^i)(k_1^2 k_{0y} + k_0^2 k_{1y})} jF(k_x - k_x^i) \quad (3.1.11)$$

being $k_{0y}^i = \sqrt{k_0^2 - (k_x^i)^2}$; $k_{1y}^i = \sqrt{k_1^2 - (k_x^i)^2}$ and $F(k_x)$ is the Fourier transform of $f(x)$. To simplify the expressions for a general rough surface, we can assume that the surface roughness is sinusoidal. For $f(x) = h \cos(\frac{2\pi}{\lambda_s}x)$, the transmitted field can be written as

$$V_t = \sum_{p=-1}^1 \tau_{0p}(k_x) e^{j(k_{0y}^i - k_{1py})d} e^{-j(k_{px}x - k_{0py}y)} \quad (3.1.12)$$

where

$$\tau_{0p}^{TM}(k_{px}) = \begin{cases} \frac{2k_{0py}}{k_{0py} + k_{1py}} & p = 0 \\ \frac{jhk_{0y}^i(k_0^2 - k_1^2)}{(k_{0y}^i + k_{1y}^i)(k_{0py} + k_{1py})} & p = \pm 1 \end{cases} \quad (3.1.13)$$

$$\tau_{0p}^{TE}(k_{px}) = \begin{cases} \frac{2k_{0py}}{k_{0py} + k_{1py}} & p = 0 \\ \frac{ihk_1^2 k_{0y}^i (k_0^2 - k_1^2) (k_{px} k_x^i - k_{0y}^i k_{0py})}{(k_1^2 k_{0y}^i + k_1^2 k_{1y}^i) (k_1^2 k_{0py} + k_0^2 k_{1py})} & p = \pm 1 \end{cases} \quad (3.1.14)$$

3.1.2 Scattering from coated cylinder

Decomposition of the total field for the scattering scenario and the multiple interactions are shown in figure 3.2(b). It is worth mentioning that the field illuminating the cylinder is not the initial incident field V_i but the field transmitted V_t into medium 1. In general, the scattered field is given by

$$V_s^{(1)} = \sum_{n=-\infty}^{\infty} j^{-n} T_n^{(1)}(k_x) \left[\hat{z} A_n H_n^{(2)}(k_1 \rho) + \hat{\phi} B_n H_n'^{(2)}(k_1 \rho) \right] e^{jn\varphi} \quad (3.1.15)$$

where A_n and B_n are mode coefficients derived in chapter 2 for CCM, chiral, plasma, and TI materials. In the above equation

$$T_n^{(1)}(k_x) = \int_{-\infty}^{\infty} \left[\tau_{01}^{(0)}(k_x) \delta(k_x - k_x^i) + \tau_{01}^{(1)}(k_x) \right] e^{j(k_{0y} - k_{1y})d} e^{-jn \tan^{-1}(\frac{-k_{1y}}{k_x})} dk_x \quad (3.1.16)$$

The reflection of the scattered field is calculated by representing the cylindrical field as plane waves and applying the PT. Equation (3.1.15) can be written as [56]:

$$V_s^{(1)} = \frac{1}{\pi} \int_{-\infty}^{\infty} \frac{1}{k_{1y}} e^{-j(k_x x + k_{1y} y)} \sum_{n=-\infty}^{\infty} \left(\hat{z} a_n - \hat{\phi} j b_n \right) T_n^{(1)}(k_x) e^{jn \tan^{-1}(\frac{k_y^1}{k_x})} dk_x \quad (3.1.17)$$

Thus, the first order field (scattered- reflected) can be written as [70]

$$V_{\text{sr}}^{(1)} = \frac{1}{\pi} \int \frac{1}{k_{1y}} \sum_{n=-\infty}^{\infty} \left(\hat{z}a_n - \hat{\phi}jb_n \right) T_n(k_x) e^{jn \tan^{-1}(\frac{k_{1y}}{k_x})} \\ \times \left\{ \int_{k'_x} \left[\gamma_{10}^{(0)}(k_x, k'_x) \delta(k'_x - k_x) + \gamma_{10}^{(1)}(k_x, k'_x) \right] e^{-j(k_{1y}+k'_{1y})d} e^{-j(k'_x x - k'_{1y} y)} dk'_x \right\} dk_x \quad (3.1.18)$$

Considering the above field as incidence, the second order interaction between the interface and the object can be described as [64]

$$V_{\text{sr}}^{(2)} = \sum_{n=-\infty}^{\infty} j^{-n} \left[\hat{z}a_n H_n^{(2)}(k_1 a) - \hat{\phi}jb_n H_n'^{(2)}(k_1 a) \right] T_n^{(2)} e^{jn\varphi} \quad (3.1.19)$$

where

$$T_n^{(2)} = (T_n^{co(2)} + T_n^{cr(2)}) \quad (3.1.20)$$

$$= \frac{1}{\pi} \sum_{m=-\infty}^{\infty} (a_m - jb_m) T_m^{(1)} I_{m,n}^{RW} \quad (3.1.21)$$

and

$$I_{m,n}^{RW} = \int \int \frac{1}{k_{1y}} \left[\gamma_{10}^{(0)}(k_x, k'_x) \delta(k'_x - k_x) + \gamma_{10}^{(1)}(k_x, k'_x) \right] \\ \times e^{-j(k_{1y}+k'_{1y})d} e^{jm \tan^{-1}(\frac{k_{1y}}{k_x})} e^{-jn \tan^{-1}(\frac{-k'_{1y}}{k'_x})} dk'_x dk_x \quad (3.1.22)$$

The q -th order scattered fields can be written as

$$V_{\text{sr}}^{(q)} = \sum_{n=-\infty}^{\infty} j^{-n} \left[\hat{z}a_n H_n^{(2)}(k_1 a) - \hat{\phi}jb_n H_n'^{(2)}(k_1 a) \right] T_n^{(q)} e^{jn\varphi} \quad (3.1.23)$$

where

$$T_n^{(q)} = \frac{1}{\pi} \sum_{m=-\infty}^{\infty} (a_m - jb_m) T_m^{(q-1)} I_{m,n}^{RW} \quad (3.1.24)$$

From equation (3.1.24), it is clear that the q th reflection can be written in terms of previous reflections. The total scattered-reflected field can be written as

$$V_{\text{sr}} = \sum_{n=-\infty}^{\infty} j^{-n} (a_n - jb_n) T_n H_n^{(2)}(k_1 \rho) e^{jn\varphi} \quad (3.1.25)$$

where

$$T_n = \sum_{q=1}^{\infty} T_n^{(q)} \quad (3.1.26)$$

After multiple reflections, the field above the rough surface can be written as

$$V_{st}^{(total)} = \frac{1}{\pi} \sum_{n=-\infty}^{\infty} (a_n - j b_n) T_n I_n^{TW} \quad (3.1.27)$$

where

$$\begin{aligned} I_n^{TW} = & \int_{k_x} \int_{k'_x} \frac{1}{k_{1y}} \left[\tau_{10}^{(0)}(k_x, k'_x) \delta(k'_x - k_x) + \tau_{10}^{(1)}(k_x, k'_x) \right] \\ & \times e^{jn \tan^{-1}(\frac{k_{1y}}{k_x})} e^{j(k_{0y} - k_{1y})d} e^{-j(k'_x x + k'_{0y} y)} dk_x \end{aligned} \quad (3.1.28)$$

Chapter 4

Numerical results and discussions

In this chapter, numerical implementation and results are presented which involves the following steps:

- the selection of a rough surface profile;
- truncation of summations to $N_t = 3k_1b$ terms [67];
- evaluation of the spectral integrals using saddle point method [71];
- calculation of number of interactions between the cylinder and the interface using the criteria $|E_{st}^{(q)} / E_{st}^{(q-1)}| << 10^{-5}$.

In section 4.1, the coating of CCM is considered and results are reported for different values of refractive index of coating material, thickness of coating, period of sinusoidal surface and admittance of PEMC core. In section 4.2, coating of chiral material is assumed and results are reported for varying the parameters such as chirality, thickness of the coating etc. In section 4.3, plasma is used as coating material while TI material is used in section 4.4. Finally, comparison between results for coatings of these materials is done.

4.1 Results for coating of CCM

Let us assume that a PEMC cylinder is coated with CCM. The results reported in [7, 64] are reproduced to confirm the validity of the formulation. Scattering patterns for

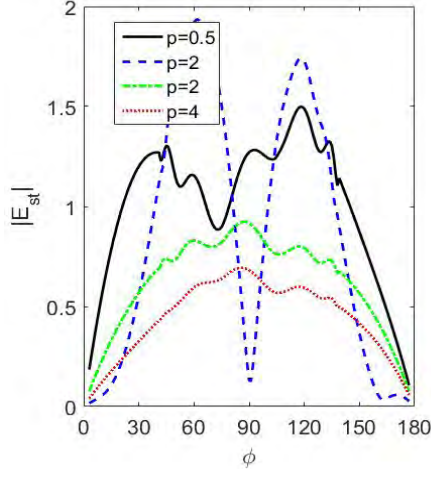
different values of real part p and imaginary part q of permittivity and permeability are shown in figures (4.1) and (4.2), respectively. The simulation parameters are shown in table (4.1). For all the results, these parameters are used and only change will be mentioned. As we change p or q , the refractive index of the coating material is changed and it affects the scattering pattern. It can be seen that scattering increases as the imaginary part of permittivity and permeability is increased and this effect is different from that the lossy dielectric case. The RCS can be increased by the use of CCM coating for both co and cross polarized scattering. In figure (4.3), scattering pattern for different values of b (thickness of coating material) is observed for $p = 1, q = 0.05$. Anomalous behavior can be observed due to interference of waves propagating inside the coating material. Figure (4.4) shows the pattern for different surface periods λ_s . The location of the lobes changes as a function of λ_s . The effect of core admittance M on the scattering is analyzed in figure (4.5). The cross polarized field tends to decrease as admittance parameter is increased. A large value of M corresponds to PEC case. From the above observations, it is concluded that the far zone RCS can be increased by increasing the refractive index of the CCM coating and the cross polarization decreases as a function of admittance M .

A good insight of the scattering phenomenon can be possible in all the directions by observing the two dimensional map of the near zone scattering presented in figure (4.6) for TM polarized incident field and TE polarized incident field is considered in figure (4.7). For the purpose of comparison, pattern for a PEMC cylinder with coating of a dielectric material with refractive index $n = \sqrt{m(p^2 + q^2)}$ is also reported. The difference between the results for the CCM and dielectric coating is not noticeable.

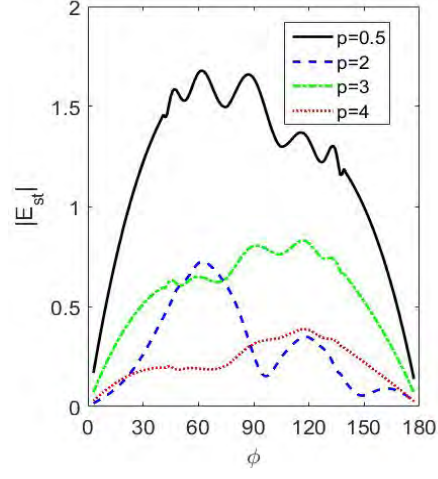
The refractive index of the coating material is increased and results have been presented in figures (4.8) and (4.9) for $p = 1$ and $q = 3$. Although the refractive index of the CCM coating is same as that of the dielectric coating, yet the distinction between the scattered fields can be noted due to different value of impedance η . A strong backward and forward scattering is noted for both components (co and cross). The field inside the coating layer is also dissimilar. These results are also helpful in understanding the change in scattering amplitude due to presence of the rough interface.

φ_i	a	b	d	A	λ_s	$M\eta$	ϵ_{r1}
-60°	$0.2\lambda_0$	$0.5\lambda_0$	$2\lambda_0$	$0.0064\lambda_0$	$0.8\lambda_0$	3	$4 - i0.01$

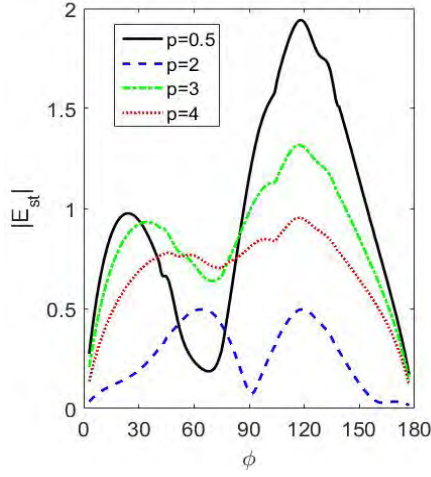
Table 4.1: Parameters for CCM coating.



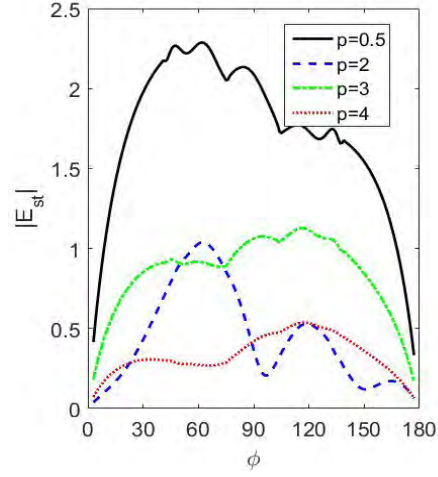
(a) Co polarized, TM



(b) Cross polarized, TM

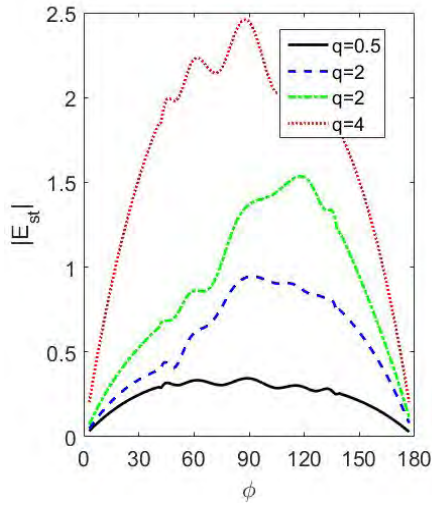


(c) Co polarized, TE

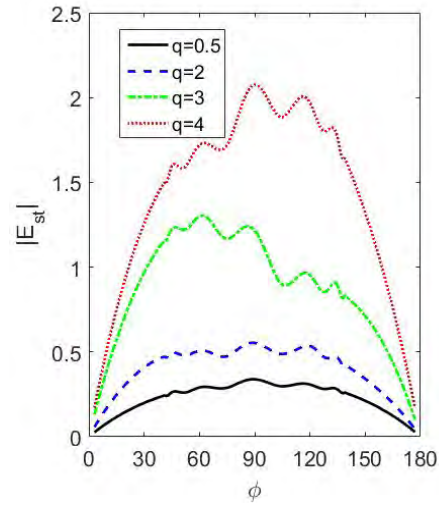


(d) Cross polarized, TE

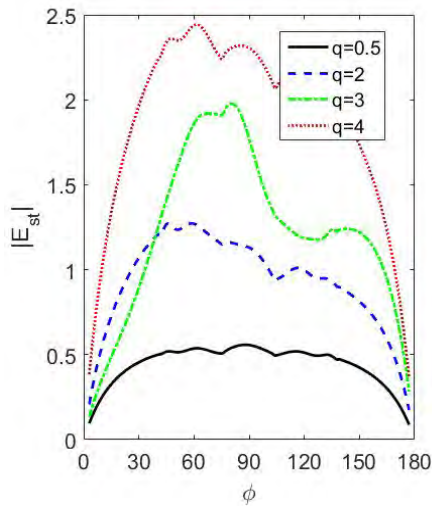
Figure 4.1: Far zone scattered field from a buried PEMC cylinder coated with CCM for different values of p , $m = 2$ and $q = 0.05$.



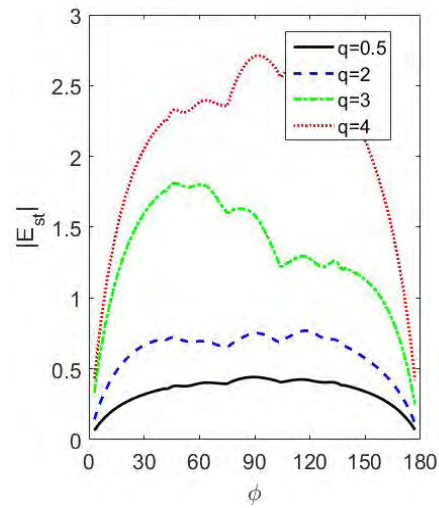
(a) Co polarized, TM



(b) Cross polarized, TM

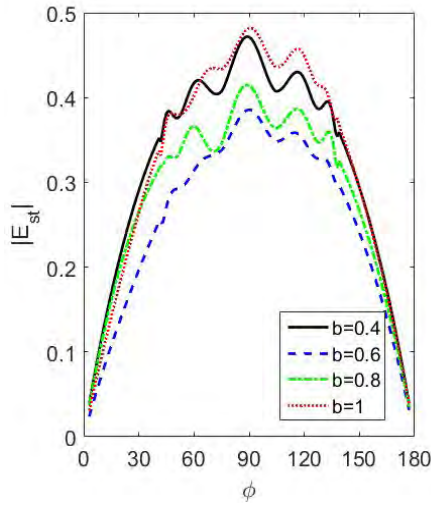


(c) Co polarized, TE

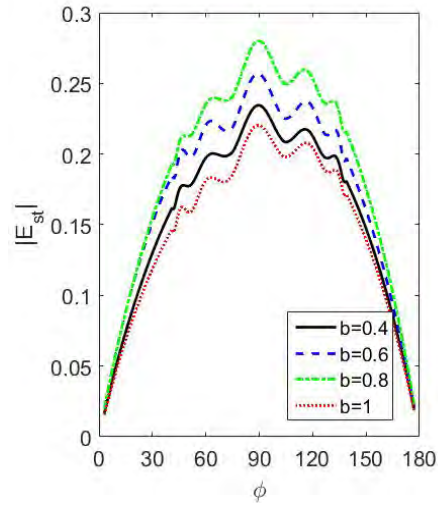


(d) Cross polarized, TE

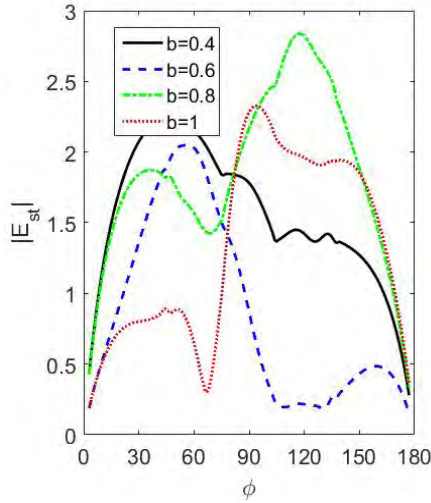
Figure 4.2: Same as figure (4.1) except that q is changed and $p=1$.



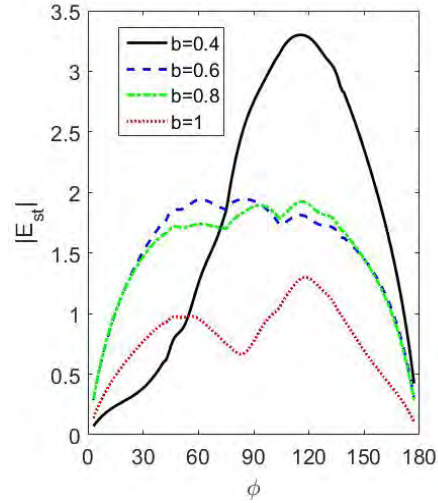
(a) Co polarized, TM



(b) Cross polarized, TM

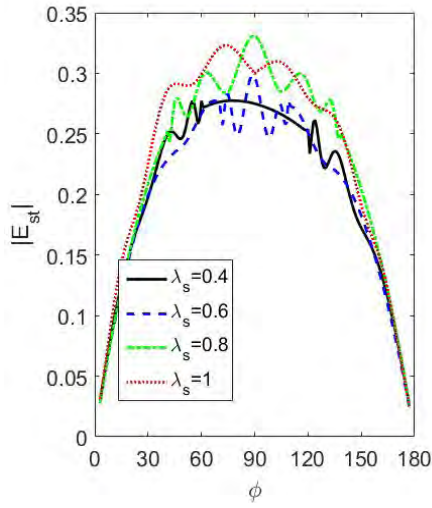


(c) Co polarized, TE

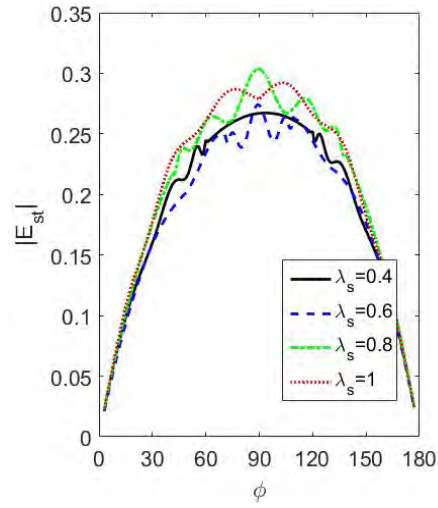


(d) Cross polarized, TE

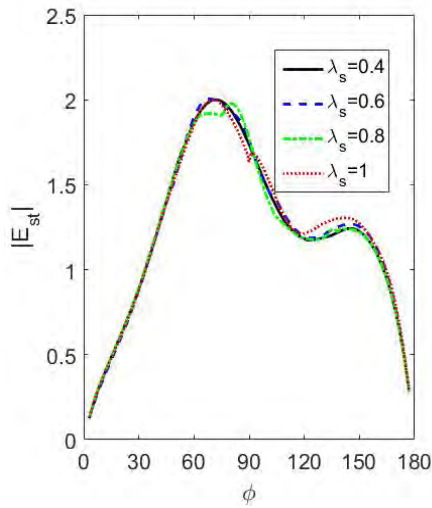
Figure 4.3: Same as figure (4.1) except that thickness of the coating material (CCM) is varied and $p = 1, q = 0.05$.



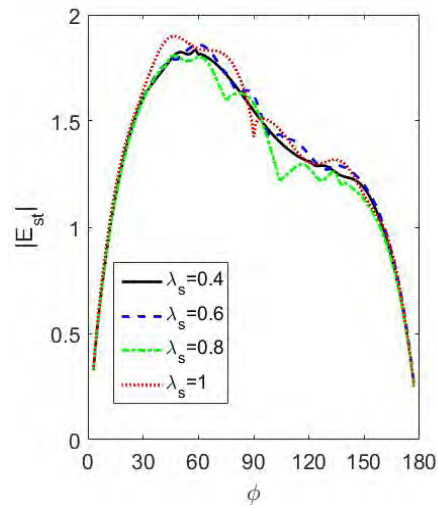
(a) Co polarized, TM



(b) Cross polarized, TM

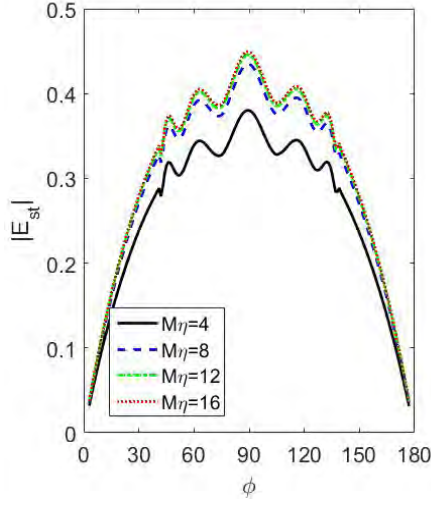


(c) Co polarized, TE

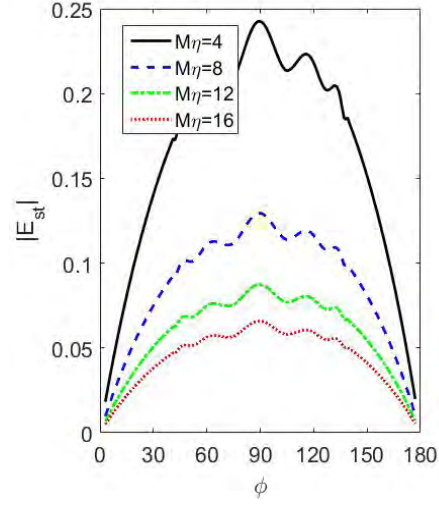


(d) Cross polarized, TE

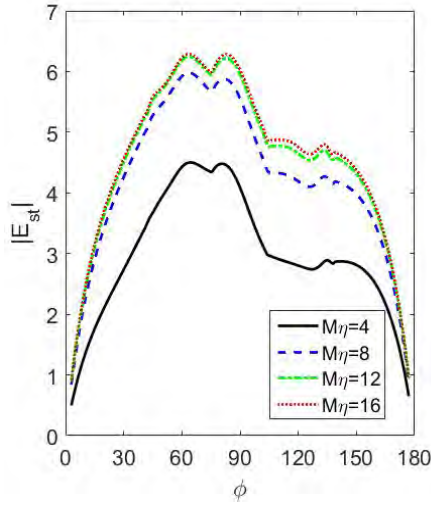
Figure 4.4: Same as figure (4.3) but for period λ_s and $b = 0.5$.



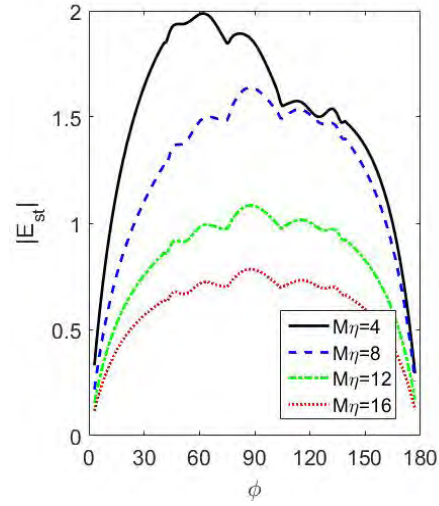
(a) Co polarized, TM



(b) Cross polarized, TM

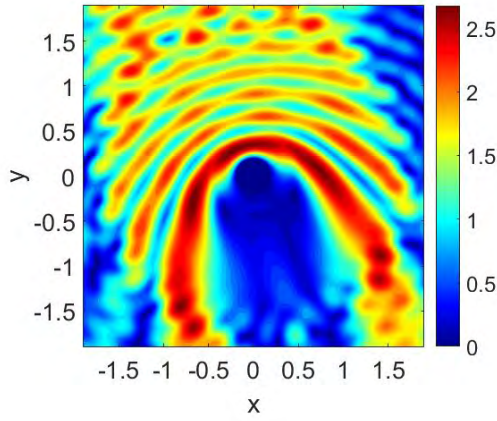


(c) Co polarized, TE

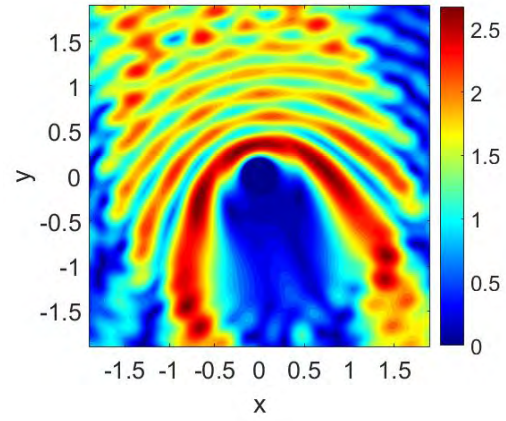


(d) Cross polarized, TE

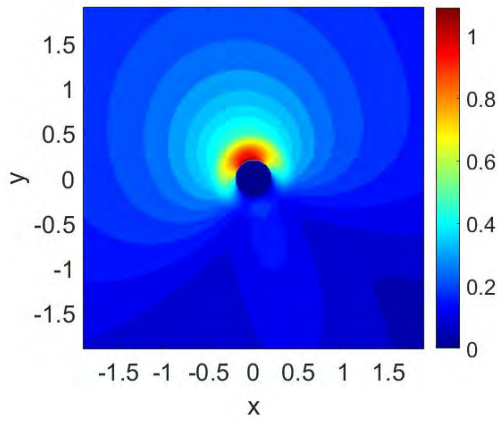
Figure 4.5: Same as figure (4.3) except that admittance M is varied.



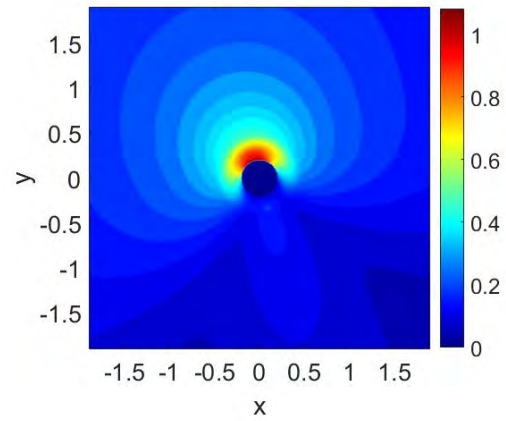
(a) Co polarized, TM, CCM



(b) Co polarized, TM, Dielectric

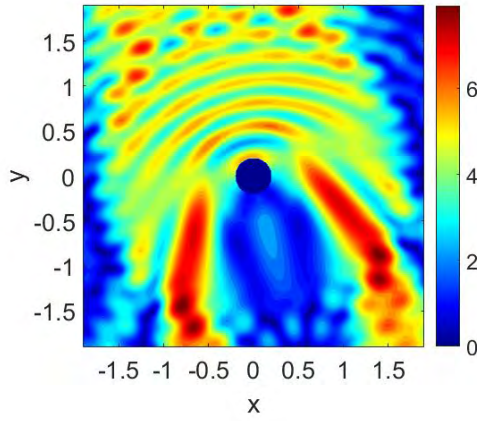


(c) Cross polarized, TM, CCM

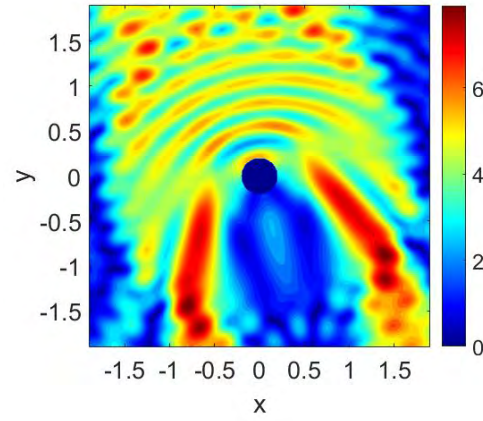


(d) Cross polarized, TM, Dielectric

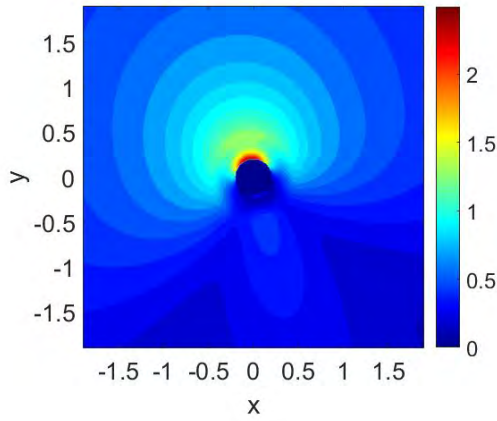
Figure 4.6: Two dimensional scattered field maps for CCM coating and TM polarized incident field.



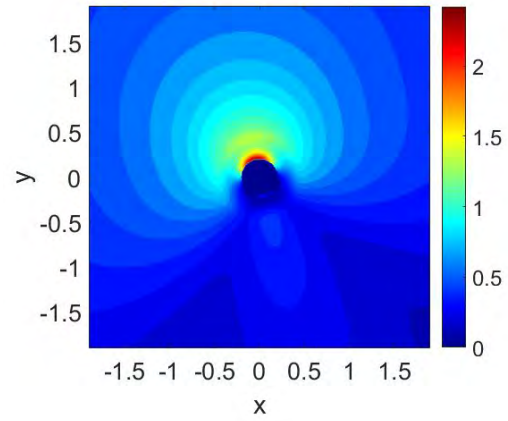
(a) Co polarized, TE, CCM



(b) Co polarized, TE, Dielectric

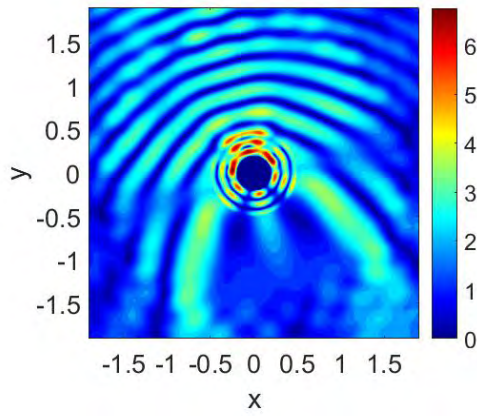


(c) Cross polarized, TE, CCM

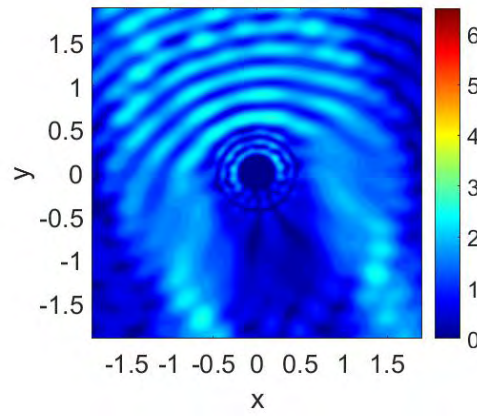


(d) Cross polarized, TE, Dielectric

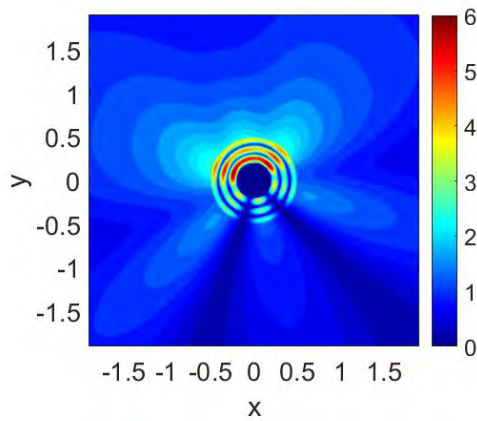
Figure 4.7: Same as figure (4.6) except that TE polarization is considered.



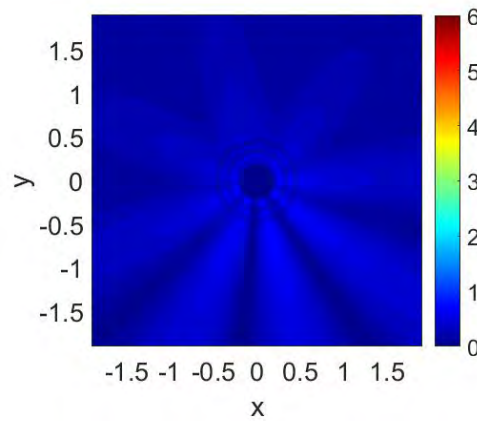
(a) Co polarized, CCM



(b) Co polarized, Dielectric



(c) Cross polarized, CCM



(d) Cross polarized, Dielectric

Figure 4.8: Same as figure (4.6) except that $q = 3$.

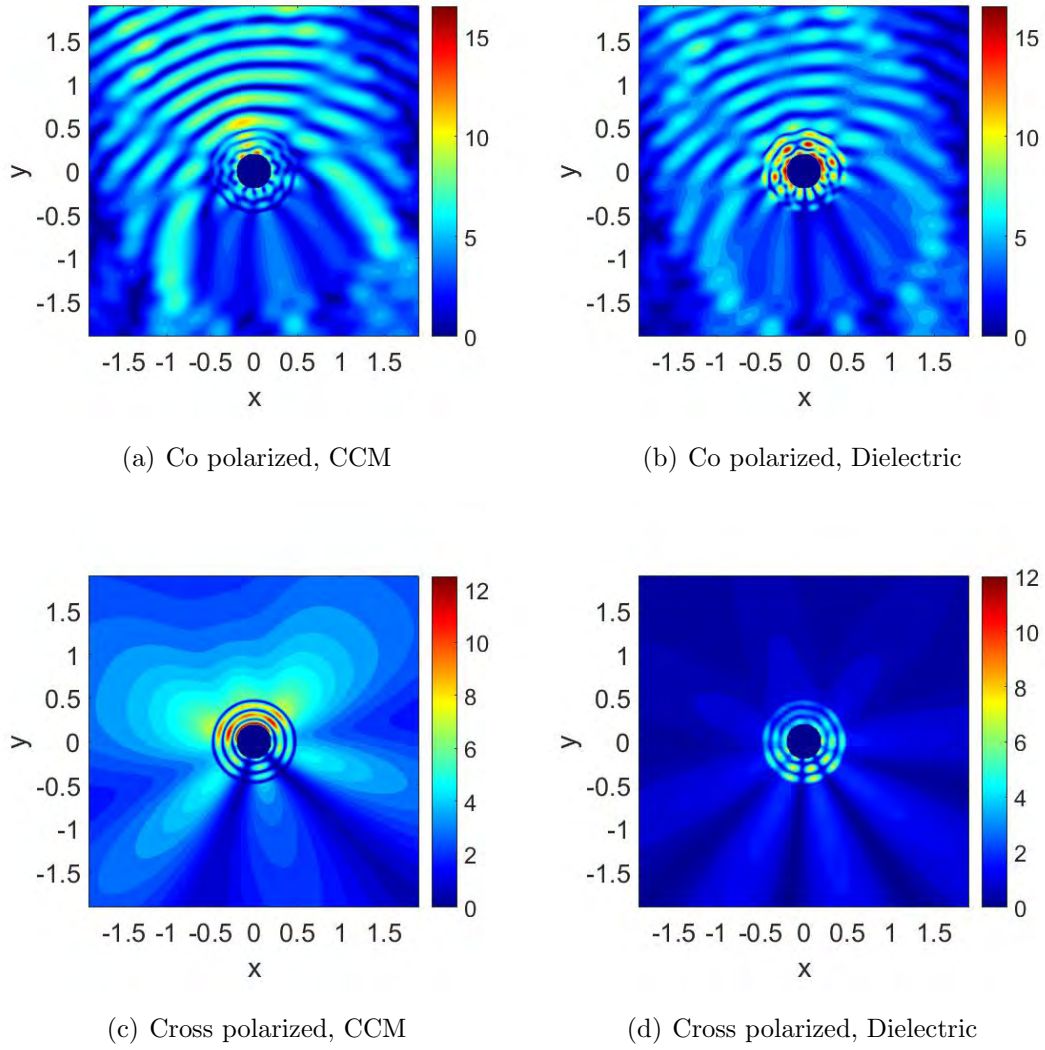


Figure 4.9: Same as figure (4.8) except that TE polarization is considered.

4.2 Results for coating of chiral material

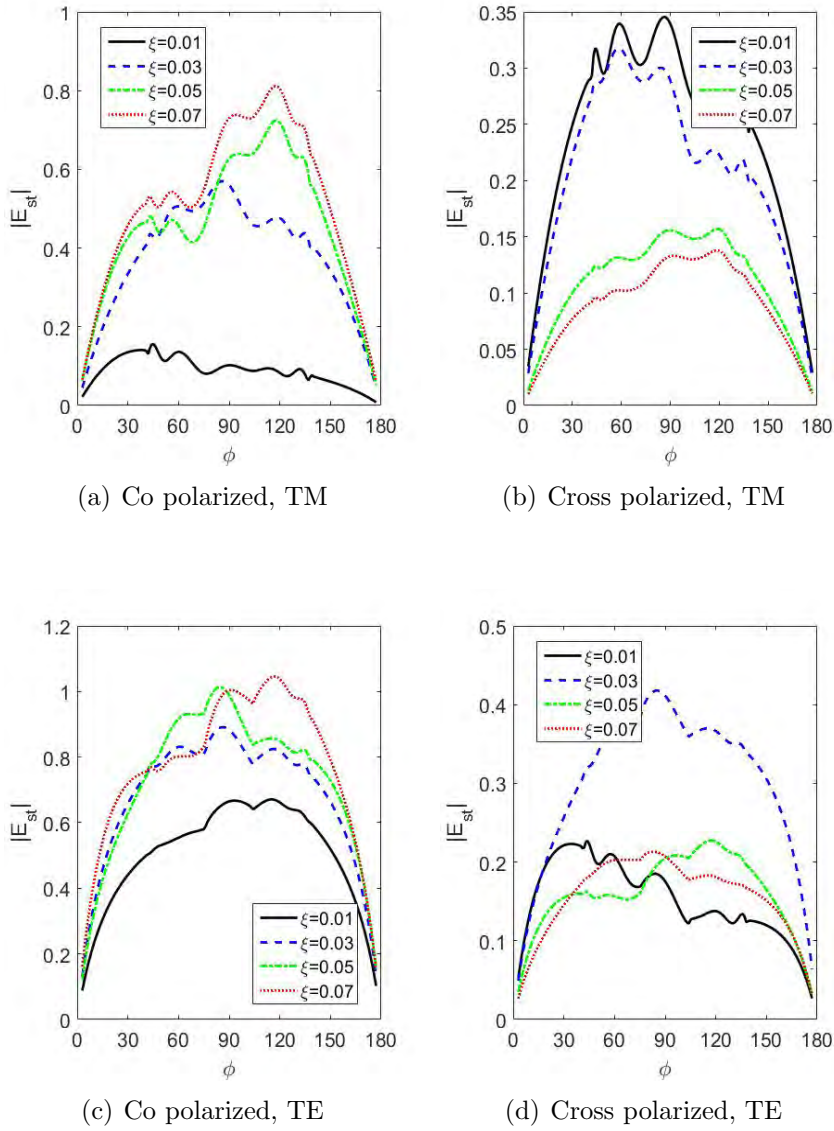
Now the coating material on PEMC core is considered to be chiral. To verify the accuracy of numerical formulation, a comparison was made between results (co polarized) obtained by using this formulation with those which are reported in figure (5) of [65]. In [65], PEC core has been used while chiral media is used as coating. Using the formulation given here and $M \rightarrow \infty$ gives results for PEC core and only three modes are selected for a sinusoidal case with proper weights.

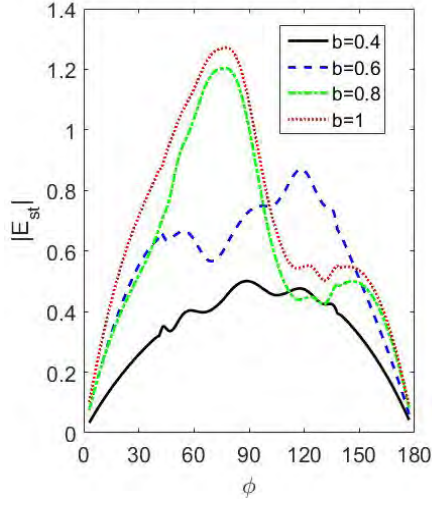
Figure (4.10) shows the field for different values of chirality of the coating material while table (4.2) shows the other parameters. The cross polarized field is small for large value of chirality in TM polarization while for TE polarized incidence, small cross polarized field is obtained for smaller value of chirality. It shows that cross polarized scattering may be altered by the coating of the chiral material. Effect of b (thickness of coating material) is shown in figure (4.11), when the value of chirality is $\xi = 0.03$. Co polarized scattering increases as chirality is increased for $\phi = [0\ 90^\circ]$. Pattern for various periods is observed in figure (4.12). The interaction between the cylinder and sinusoidal surface changes as period is changed and this effect can be clearly observed both for co as well cross polarized scattering. Moreover, the different scattering behavior is obtained for TM incident field compared to TE polarized field. The admittance M is changed in figure (4.13) to see its effect on the scattering behavior. It shows that scattering for PEC core is less than that for PEMC core in case TE polarized field is incident while the core has not significant effect on scattering for TM polarized excitation.

Near zone two dimensional scattering pattern is shown in figure (4.14) for TM and TE polarized incident fields. The difference between the results for both polarization states is quite noticeable and low cross polarized intensity is found for TM polarized illumination. Comparing figure (4.14) with figures (4.6), (4.7) for the dielectric coating, the difference between scattering patterns shows the effect of chirality.

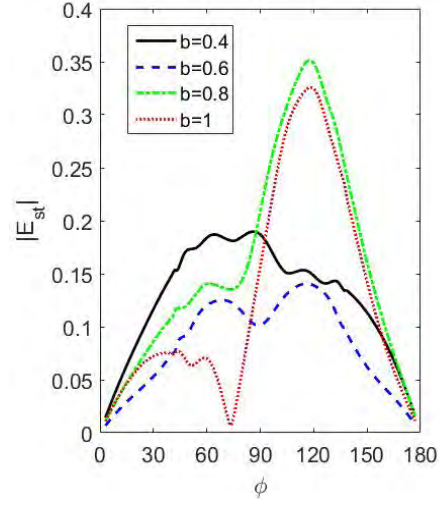
φ_i	a	b	d	A	λ_s	$M\eta$	ϵ	μ	ϵ_{r1}
-60°	$0.2\lambda_0$	$0.5\lambda_0$	$2\lambda_0$	$0.0064\lambda_0$	$0.8\lambda_0$	3	2.25	1	$4 - i0.01$

Table 4.2: Parameters for coating of chiral material.

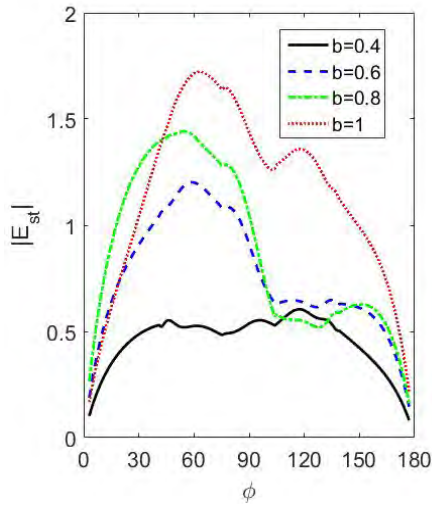
Figure 4.10: Far zone scattered field for the coating of chiral material as a function of chirality ξ .



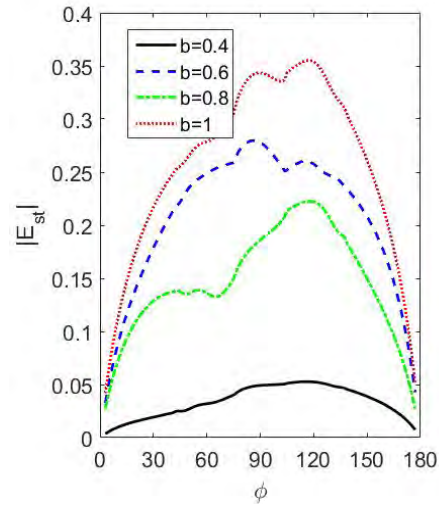
(a) Co polarized, TM



(b) Cross polarized, TM

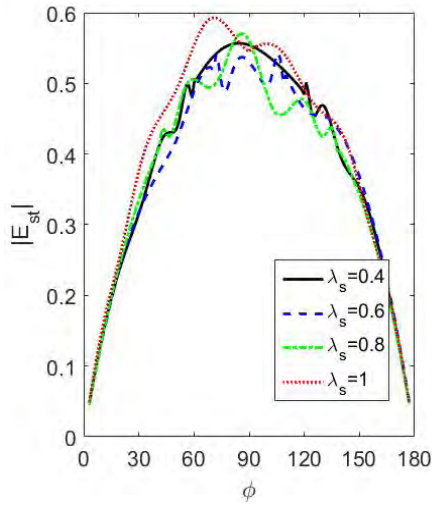


(c) Co polarized, TE

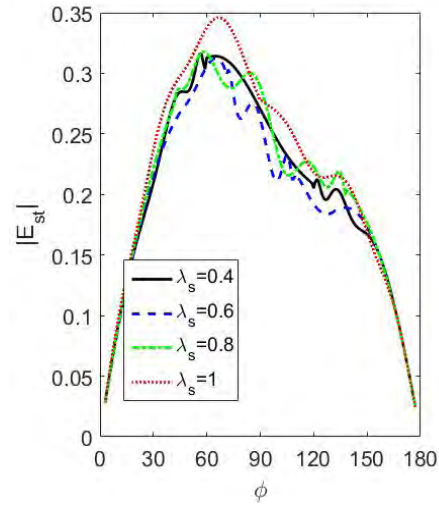


(d) Cross polarized, TE

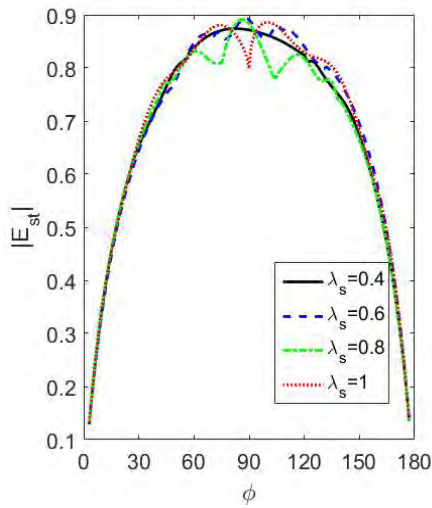
Figure 4.11: Same as figure (4.10) except that thickness b is changed and $\xi = 0.03$.



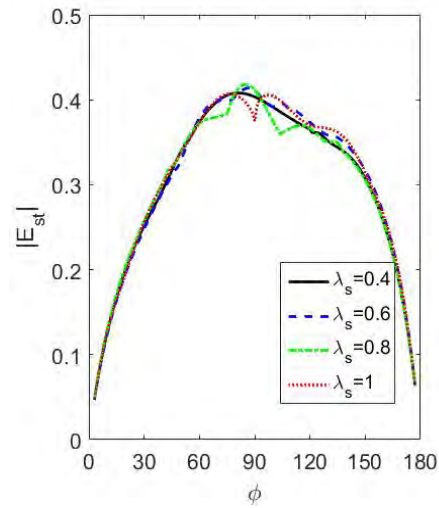
(a) Co polarized, TM



(b) Cross polarized, TM

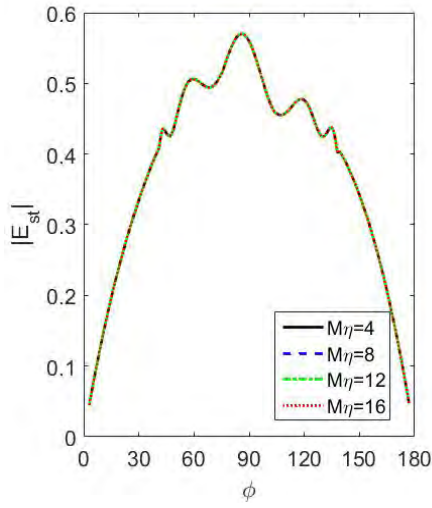


(c) Co polarized, TE

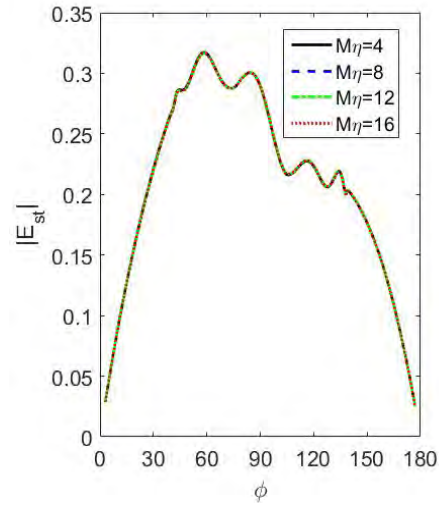


(d) Cross polarized, TE

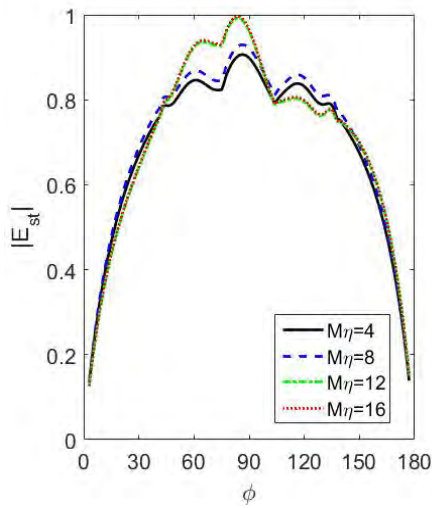
Figure 4.12: Same as figure (4.11) but for different periods λ_s and $b = 0.5$.



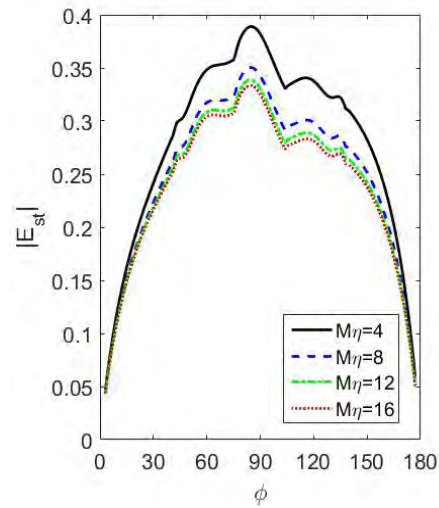
(a) Co polarized, TM



(b) Cross polarized, TM

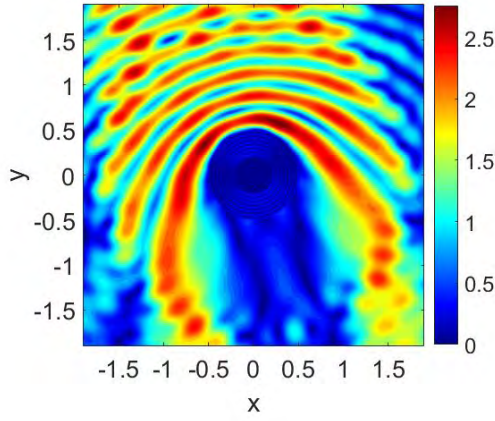


(c) Co polarized, TE

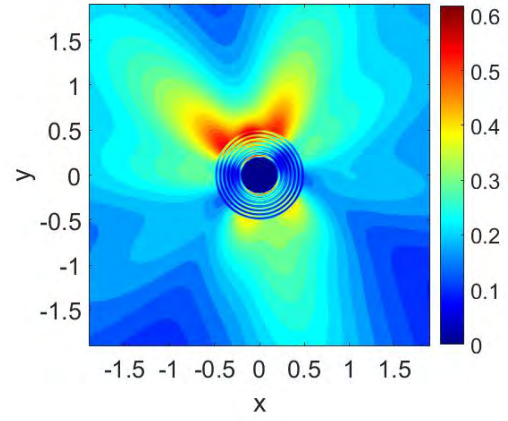


(d) Cross polarized, TE

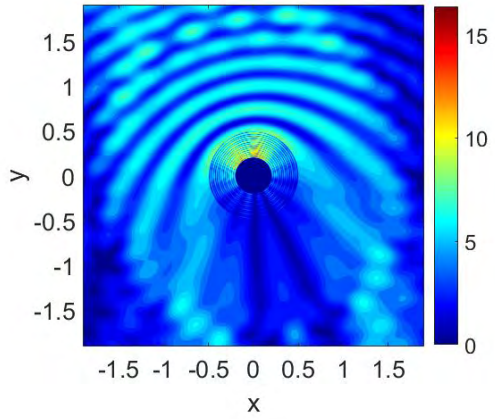
Figure 4.13: Same as figure (4.11) except that admittance M is varied.



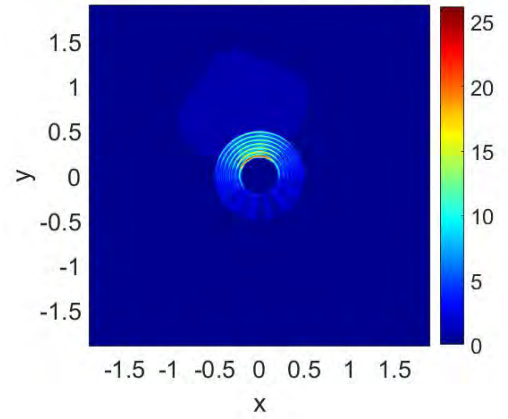
(a) Co polarized, TM, Chiral



(b) Cross polarized, TM, Chiral



(c) Co polarized, TE, Chiral



(d) Cross polarized, TE, Chiral

Figure 4.14: Two dimensional scattered field maps for coating of chiral material.

4.3 Results for coating of plasma material

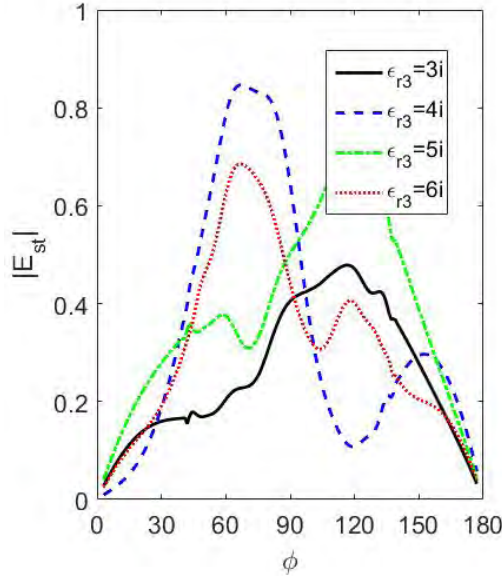
Now plasma material is used as coating material. To validate the numerical implementation, a comparison with MOM was done first [68]. The case of a PEC cylinder buried below a flat interface is obtained by putting the permittivity of the coating layer equal to that of hosting medium in the numerical code.

Scattering pattern for different values of ϵ_{r3} is shown in figure (4.15) with parameters presented in table (4.3). The effect of anisotropy can clearly be observed both polarizations. Figure (4.16) shows the pattern for different values of b and $\epsilon_{r3} = 3i$. As thickness is increased, the cross polarized component increases. The period of surface is changed in figure (4.17). The admittance of the core has been changed in figure (4.18) to observe its effect on the scattering behavior. For PEC core (large value of admittance), the cross polarization is minimum while it is maximum for small values of admittance.

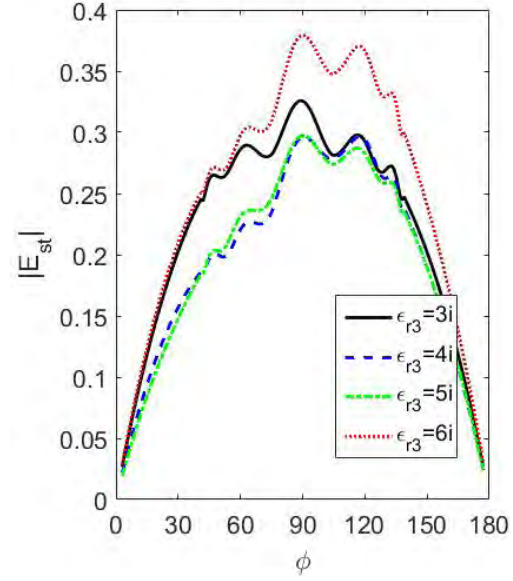
Figure (4.19) presents the two dimensional scattering field map for both TM and TE polarized incident field. Very low forward scattering is observed for cross polarized field while backward scattering is significant. A comparison with figures (4.6), (4.7) for isotropic dielectric material reveals the effect of anisotropy in backward and forward scattering properties.

φ_i	a	b	d	A	λ_s	$M\eta$	ϵ_{r1}	ϵ_{r2}	μ_{r1}, μ_{r2}	ϵ_{r4}
-60°	$0.2\lambda_0$	$0.5\lambda_0$	$2\lambda_0$	$0.0064\lambda_0$	$0.8\lambda_0$	3	$4 - i0.01$	2.25	1	5

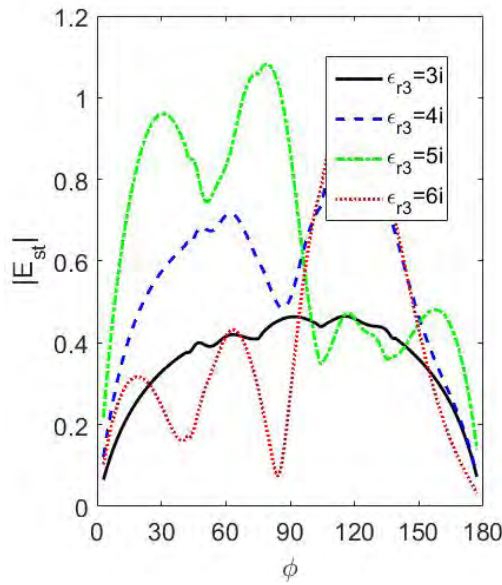
Table 4.3: Parameters for the coating of plasma material.



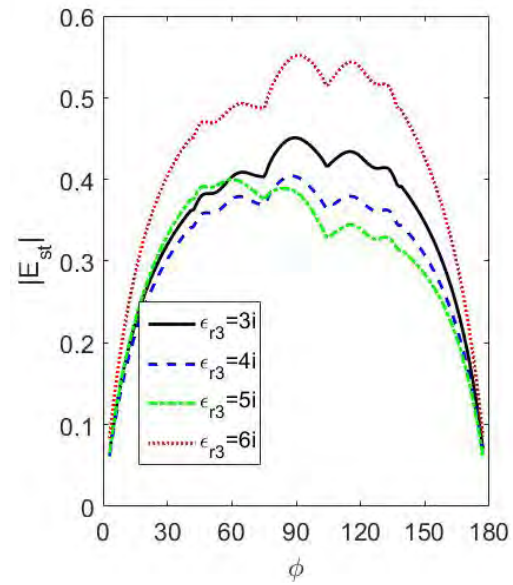
(a) Co polarized, TM



(b) Cross polarized, TM

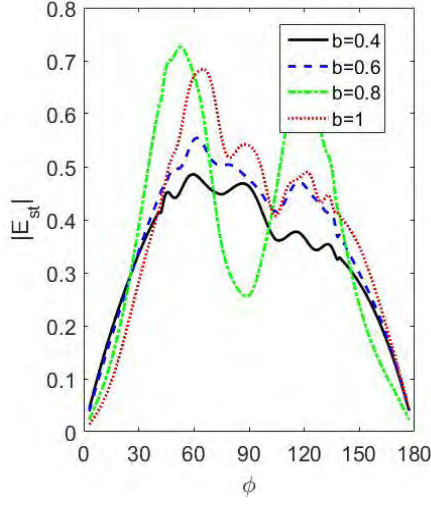


(c) Co polarized, TE

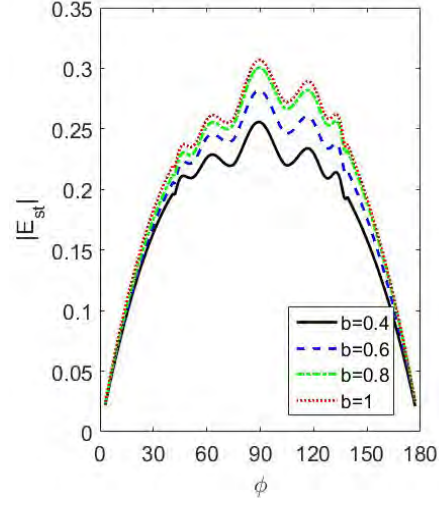


(d) Cross polarized, TE

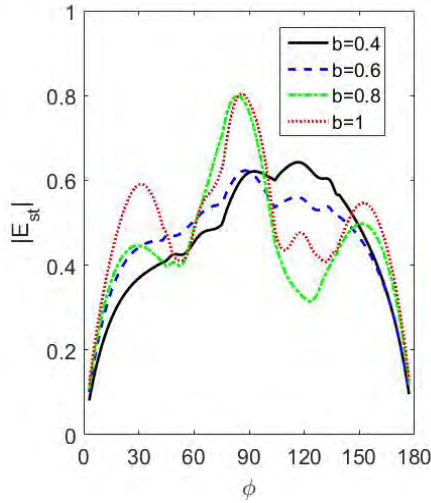
Figure 4.15: Far zone scattered field for the coating of plasma material for different values of ϵ_{r3} .



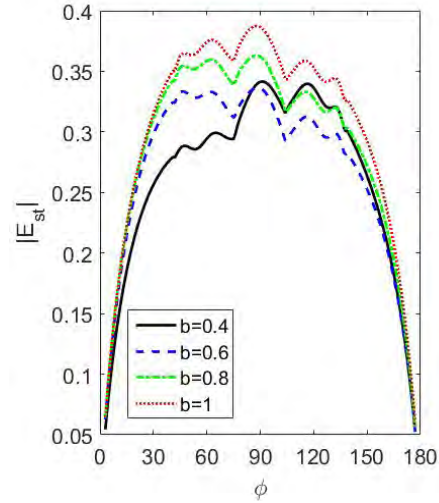
(a) Co polarized, TM



(b) Cross polarized, TM

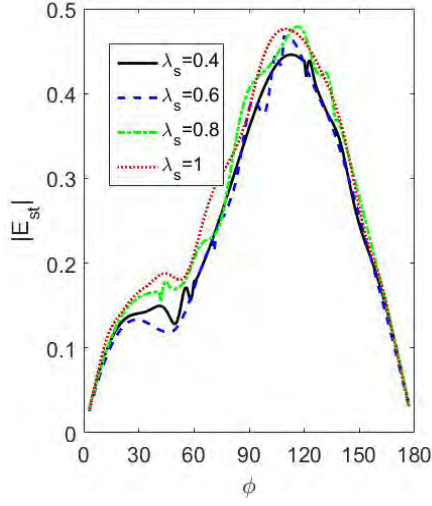


(c) Co polarized, TE

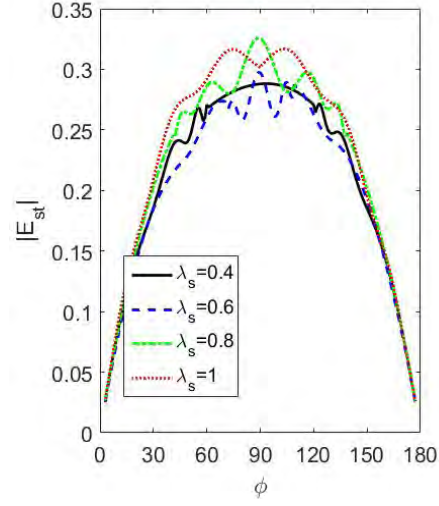


(d) Cross polarized, TE

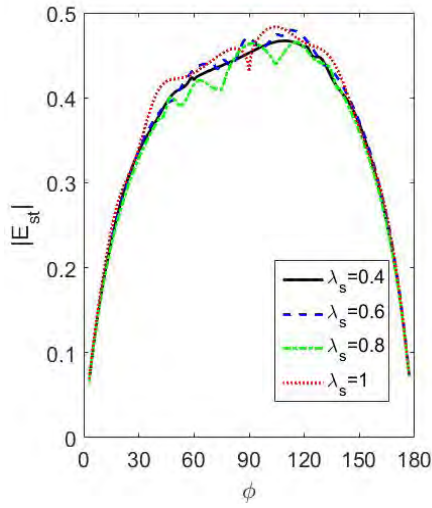
Figure 4.16: Same as figure (4.15) with $\epsilon_{r3} = 3i$ and for different values of thickness of coating b .



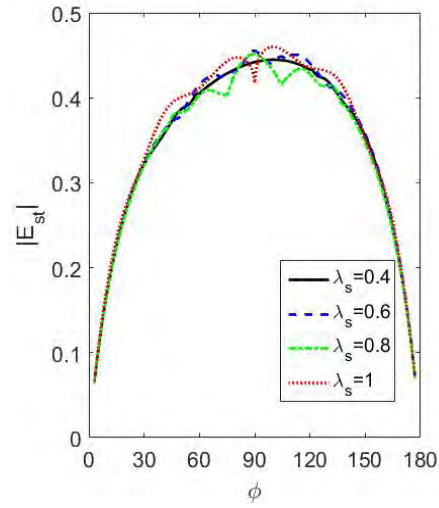
(a) Co polarized, TM



(b) Cross polarized, TM

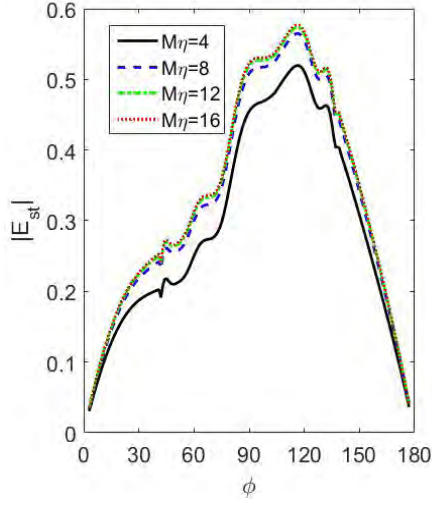


(c) Co polarized, TE

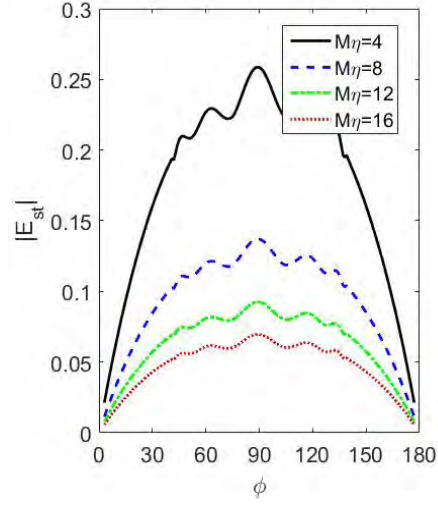


(d) Cross polarized, TE

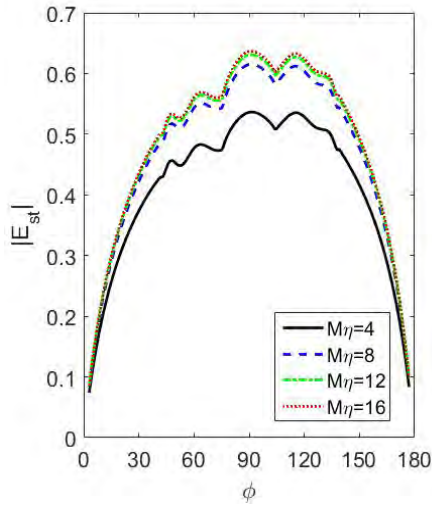
Figure 4.17: Same as figure (4.16) except that λ_s is changed and $b = 0.5$.



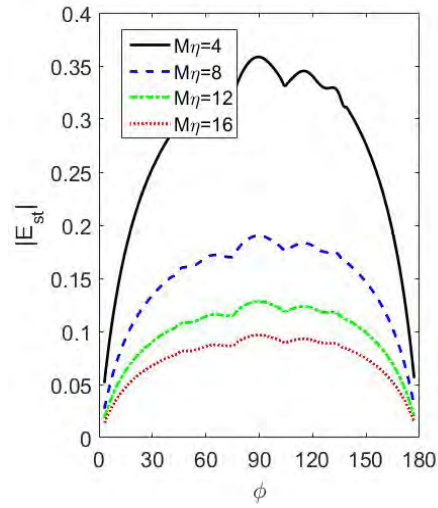
(a) Co polarized, TM



(b) Cross polarized, TM

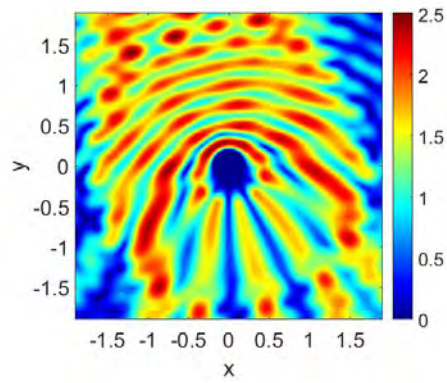


(c) Co polarized, TE

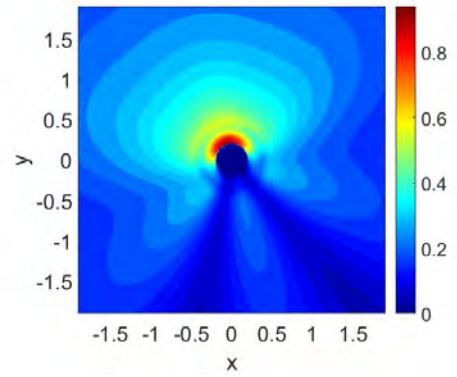


(d) Cross polarized, TE

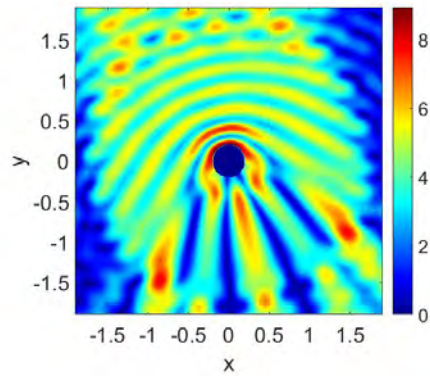
Figure 4.18: Same as figure (4.16) but results are shown for M .



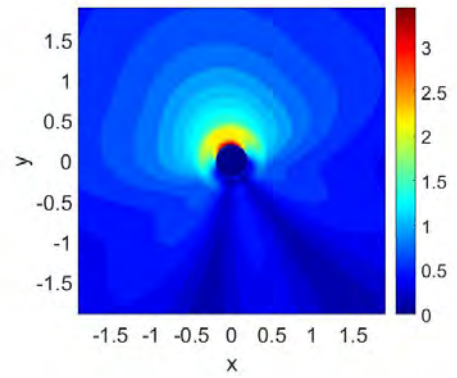
(a) Co polarized, TM, plasma



(b) Cross polarized, TM, plasma



(c) Co polarized, TE, plasma



(d) Cross polarized, TE, plasma

Figure 4.19: Two dimensional scattered field maps for the coating of plasma material.

4.4 Results for coating of topological insulator material

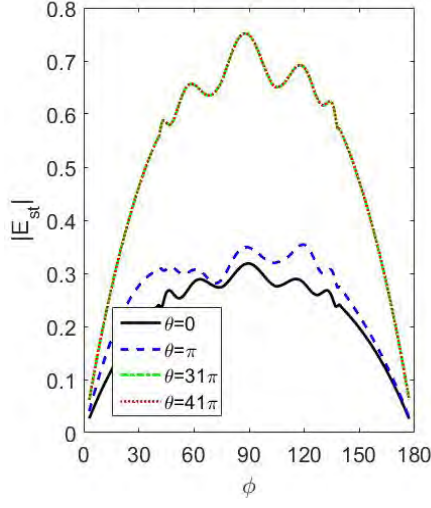
Finally, the coating material of PEMC cylinder is considered to be topological insulator material. Scattering pattern for different magneto-electric parameters is shown in figure 4.20. The simulation parameters are reported in table 4.4. As TRS is broken $\theta = 41\pi$, cross polarized scattering becomes small for TM polarization. The variation is not significant for TE polarization as observed in [66, 42].

Figure 4.21 shows the effect of thickness of coating material on the scattered field while period of surface is changed in figure (4.22) for $\theta = 41\pi$. The admittance of the core M has been changed in figure (4.23). It has no effect on scattering for TM incidence. The small strength of cross polarized component is noted for PEC core when TE polarized field is incident. As M decreases, the cross polarization increases.

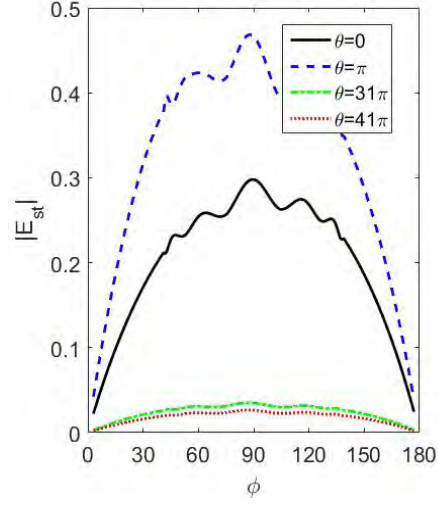
Near zone two dimensional scattering field map is analyzed in figure 4.24. From the comparison between results for two polarizations, it can be noted that cross polarized scattering can be reduced for TM polarization. Moreover, for TM polarization, the forward and backward scattering properties are different from that for the TE polarization. The comparison between TI field maps in figure 4.24 and dielectric field maps given in figures (4.6), (4.7) shows effect of magneto-electric coupling.

φ_i	a	b	d	A	λ_s	$M\eta$	ϵ_{r1}	ϵ_r	μ_{r1}, μ_r
-60°	$0.2\lambda_0$	$0.5\lambda_0$	$2\lambda_0$	$0.0064\lambda_0$	$0.8\lambda_0$	3	$4 - i0.01$	2.25	1

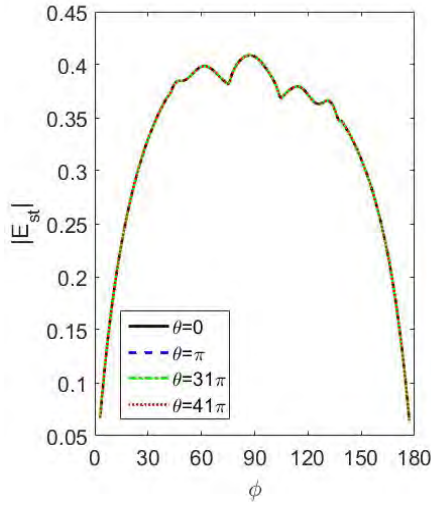
Table 4.4: Parameters for the coating of TI material.



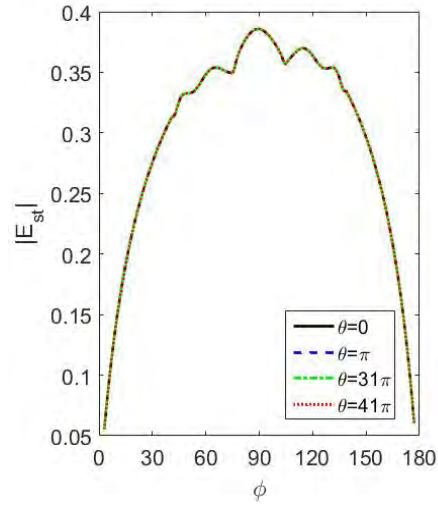
(a) Co polarized, TM



(b) Cross polarized, TM

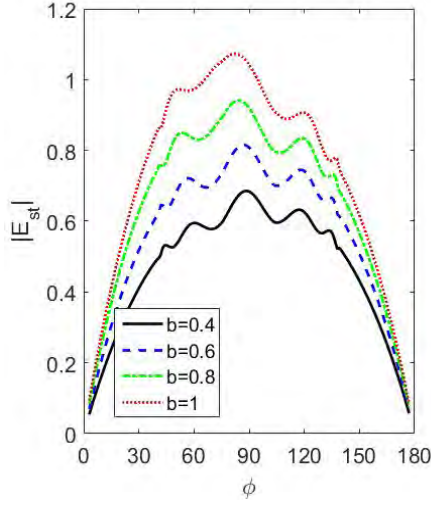


(c) Co polarized, TE

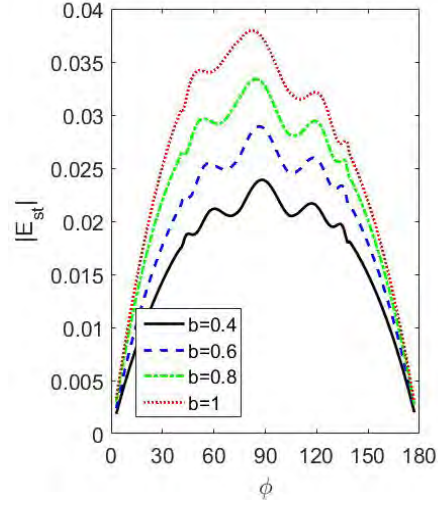


(d) Cross polarized, TE

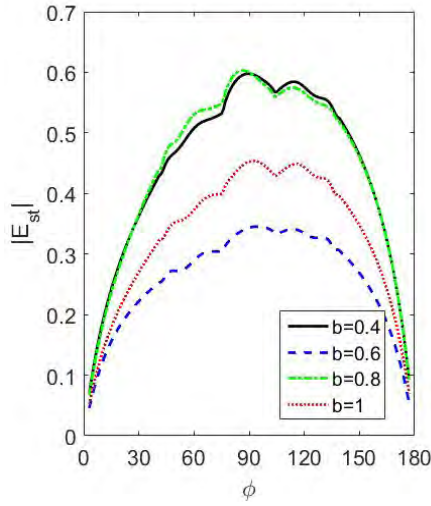
Figure 4.20: Far zone scattered field for the coating of TI material as a function of magneto-electric parameter θ .



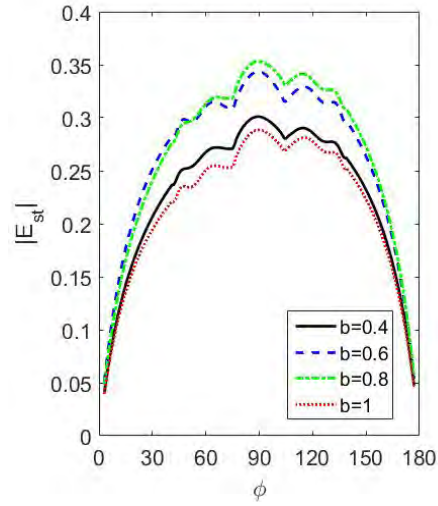
(a) Co polarized, TM



(b) Cross polarized, TM

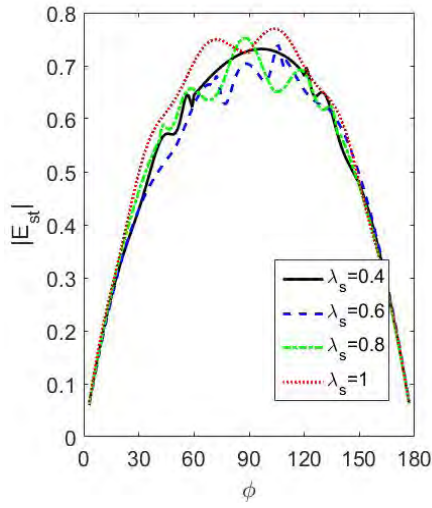


(c) Co polarized, TE

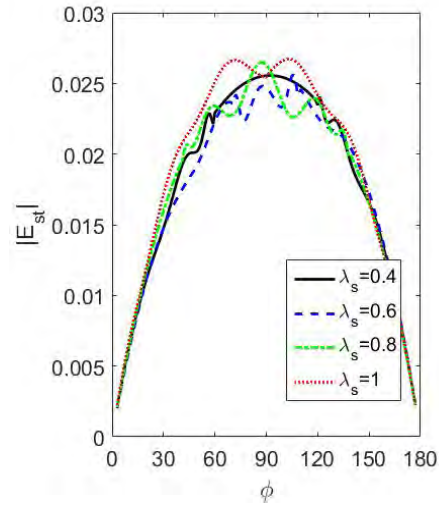


(d) Cross polarized, TE

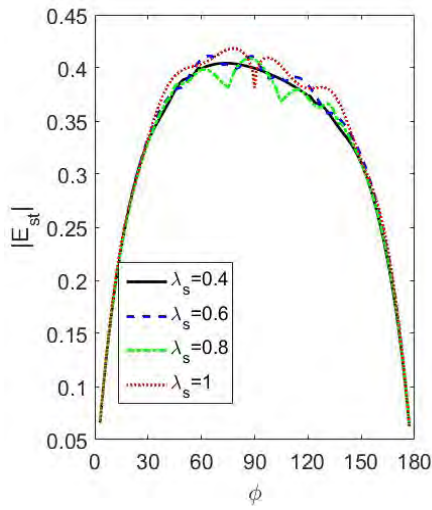
Figure 4.21: Same as figure (4.20) but for b (thickness of coating material) and $\theta = 41\pi$.



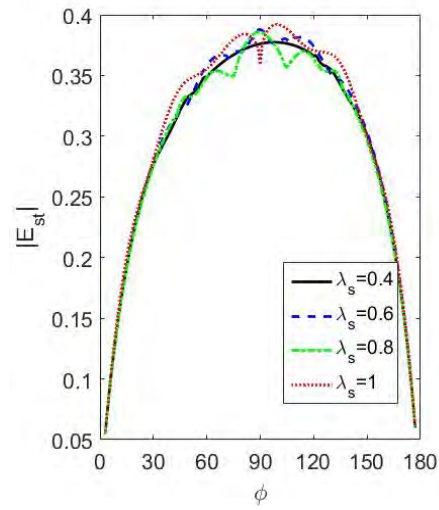
(a) Co polarized, TM



(b) Cross polarized, TM

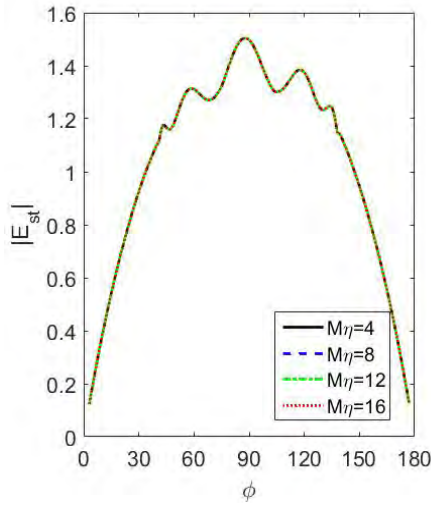


(c) Co polarized, TE

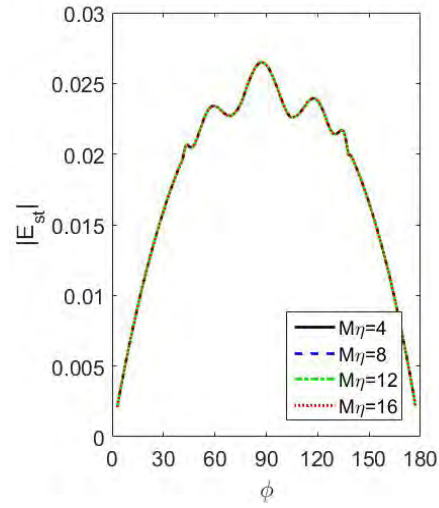


(d) Cross polarized, TE

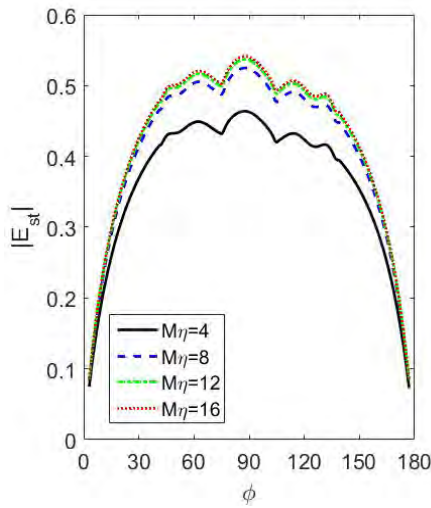
Figure 4.22: Same as figure (4.21) but for λ_s and $b = 0.5$.



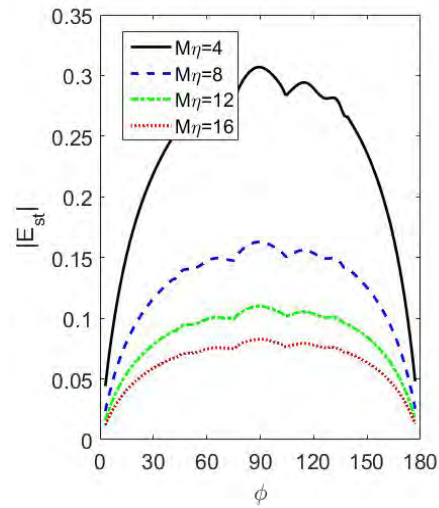
(a) Co polarized, TM



(b) Cross polarized, TM

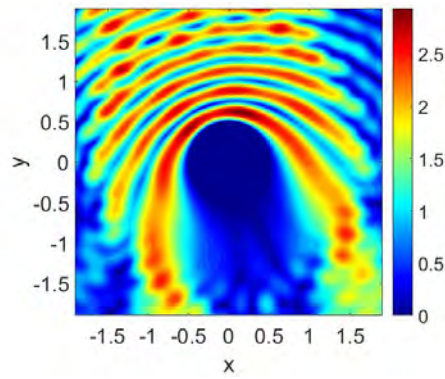


(c) Co polarized, TE

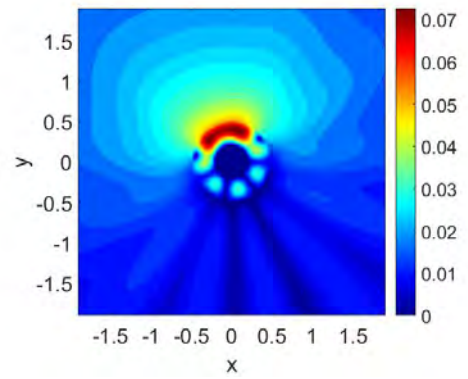


(d) Cross polarized, TE

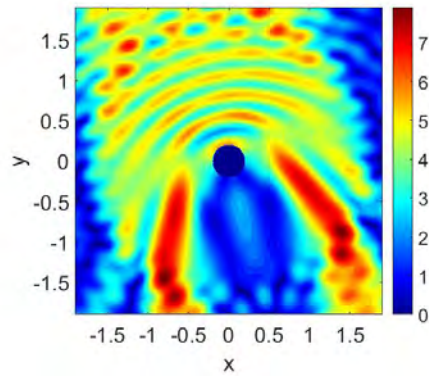
Figure 4.23: Same as figure (4.21) except that M is changed.



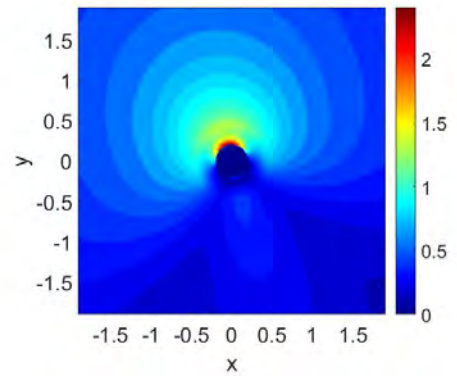
(a) Co polarized, TM



(b) Cross polarized, TM



(c) Co polarized, TE



(d) Cross polarized, TE

Figure 4.24: Two dimensional scattered field maps for the coating of TI material.

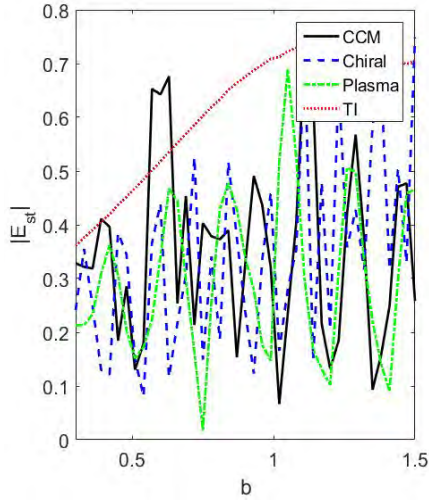
4.4.1 Comparison

Consider a PEMC material coated with CCM, chiral, plasma and TI materials. Figure (4.25) presents the variation of scattered field as a function of thickness of coating material for $p = 1, q = 0.05, \xi = 0.03, \epsilon_{r3} = 3j, \epsilon_{r4} = 5, \theta = 41\pi$. The parameters of the problem are reported in table (4.5). From the previous sections, it is noted that these parameters give small value of cross polarized scattering. The observation angle is $\phi = 30^\circ$ (bi-static case). It is noted that cross polarized field is small for the coating of TI material both for TM and TE polarized incident fields. To maximize the co polarized scattering, coating of CCM can be utilized. The amount of reduction also depends upon the polarization of the incident field and other physical/geometrical parameters. Figure (4.26) shows the result for $\phi = 120^\circ$ (mono-static) and same observation can be noted.

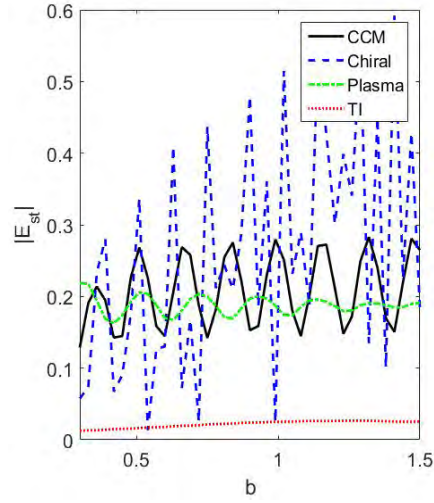
φ_i	a	b	d	A	λ_s	$M\eta$	ϵ_{r1}
-60°	$0.2\lambda_0$	$0.5\lambda_0$	$2\lambda_0$	$0.0064\lambda_0$	$0.8\lambda_0$	3	$4 - j0.01$

ϵ_r	p, q	ξ	ϵ_{r3}	θ
2.25	1, 0.05	0.03	$3j$	41π

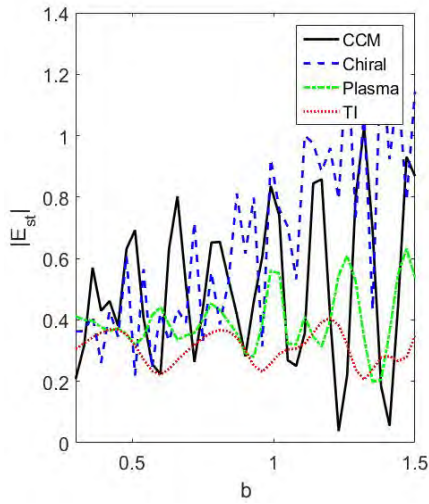
Table 4.5: Parameters for comparison of different coating materials.



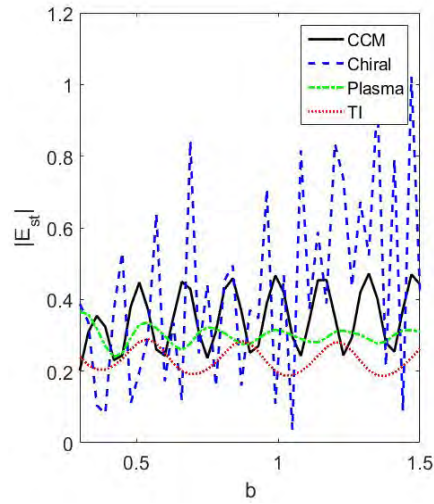
(a) Co polarized, TM



(b) Cross polarized, TM

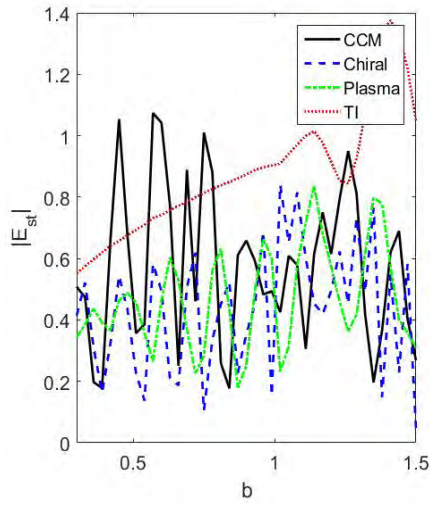


(c) Co polarized, TE

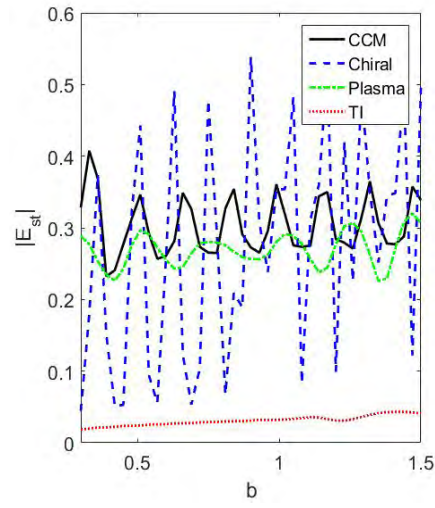


(d) Cross polarized, TE

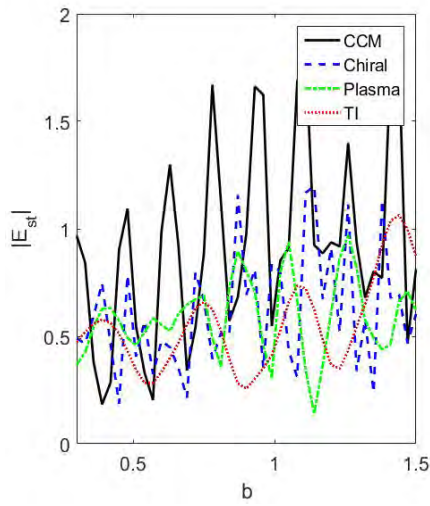
Figure 4.25: Variation of scattering as a function of thickness of the coating at $\phi = 30^\circ$.



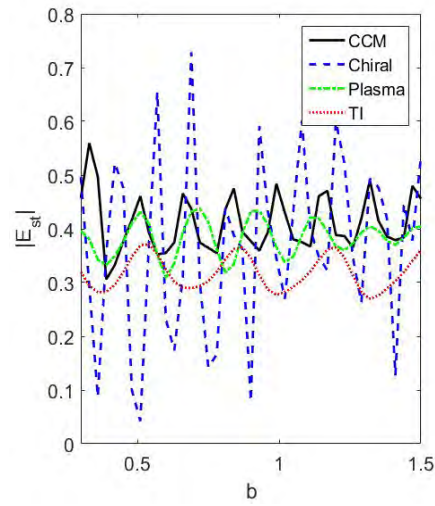
(a) Co polarized, TM



(b) Cross polarized, TM



(c) Co polarized, TE



(d) Cross polarized, TE

Figure 4.26: Same as figure 4.25 except that $\phi = 120^\circ$ is considered

Conclusion

A theoretical formulation was presented to calculate the field scattered from a buried PEMC cylinder coated with different materials such as CCM, chiral, plasma, and TI materials. Expansion of cylindrical wave functions into plane waves and perturbation theory were used to calculate the multiple reflections between coated cylinder and rough surface. Numerical implementation of the presented theory was done based on the selection of a rough surface profile, truncation of summations, solution of spectral integrals and calculation of multiple reflections using the suggested criteria. Analytical expressions of scattered field were derived and plotted.

First, near and far zone scattered fields for the coating of CCM were studied. Near zone field maps for CCM coated cylinder were compared with that of a dielectric coated cylinder and difference between back scattering and forward scattering was noted. Far zone scattering patterns were also reported by varying the involved parameters, i.e., thickness of the coating layer, period of rough surface and admittance of PEMC core.

Secondly, scattered fields for the chiral coating were evaluated and the co and cross polarized behavior of scattering was analyzed by varying the chirality and other parameters. An effort was made to study the effect of chirality by comparing near zone scattering for the coating of chiral and dielectric materials.

Thirdly, the field scattered by cylinder coated with plasma material was analyzed. Comparing the results with those obtained for the dielectric coating gives the difference due to anisotropy. Other parameters were also changed to analyze the pattern for both polarizations.

Finally, TI material is used as coating and the cases of time reversal symmetry and symmetry broken are discussed. It is observed that cross polarization is minimum for TI coating and this fact is also confirmed while comparison was done between the backward/forward scattering for the coating of different materials as a function of thickness. The amount of reduction depends on the polarization of the incident field, and other involved parameters. Moreover, it is noted that the CCM is good for making the co polarized scattering large compared to cross polarized scattering. A very good future work may be an attempt to solve this problem using the optimization techniques.

References

- [1] R.F. Harrington, *Time-Harmonic Electromagnetic Fields*, McGraw-Hill Book Co., New York, 1961.
- [2] C.A. Balanis, *Advanced Engineering Electromagnetics*, Wiley, New York, 2012.
- [3] A. Z. Elsherbeni, and M. Hamid, “Scattering by parallel conducting circular cylinders,” *IEEE Trans. Antennas Propagat.*, Vol. 35, pp. 355-358, 1987.
- [4] J.R. Wait, “Scattering of a plane wave from a circular dielectric cylinder at oblique incidence,” *Can. J. Phys.*, Vol. 33, pp. 189-195, 1955.
- [5] J.H. Richmond, “Scattering by a dielectric cylinder of arbitrary crosssection shape,” *IEEE Trans. Antennas Propagat.*, Vol.13, pp. 334-341, 1965.
- [6] B. H. Henin, A. Z. Elsherbeni, and M. Al Sharkawy, “Oblique incidence plane wave scattering from an array of circular dielectric cylinders,” *Progress In Electromagnetics Research, PIER* Vol, 68, 261–279, 2007.
- [7] A. Illahi, M. Bashir, P. Iftikhar, Q. A. Naqvi, A. Ghuffar, M. Y. Naz, A. Ghaffar, “Electromagnetic scattering from complex conjugate cylinder of infinite length,” *Journal of optoelectronics and advanced materials*, Vol. 21, pp. 338-342, 2019.
- [8] D. Dragoman, “Complex conjugate media: Alternative configuration for miniaturized lasers,” *Optics communications*, Vol. 284, pp. 2095-2098, 2011.

- [9] A. Sihvola, "Metamaterials in electromagnetics," *Metamaterials*, Vol. 1, 2-11, 2007.
- [10] V. G. Veselago, "The electrodynamics of substances with simultaneously negative values of ϵ and μ ," *Sov. Phys. Usp.*, Vol. 10, pp. 509-514, 1968.
- [11] B. H. Henin, M. H. Al Sharkawy, and A. Z. Elsherbeni, "Scattering of obliquely incident plane wave by an array of parallel concentric metamaterial cylinders," *Progress In Electromagnetics Research*, PIER Vol. 77, pp. 285-307, 2007.
- [12] A. Shooshtari and A. R. Sebak, "Electromagnetic scattering by parallel metamaterial cylinders," *Progress In Electromagnetics Research*, Vol. 57, pp. 165-177, 2006.
- [13] R. A. Shelby, D. R. Smith, and S. Schultz, "Experimental verification of a negative index of refraction." *Science*, Vol. 292, No. 5514, pp.77-79, 2001.
- [14] M. Al-Kanhal, E. A. Arvas, "Electromagnetic scattering from a chiral cylinder of arbitrary cross section," *IEEE Transactions on Antennas and Propagation*, Vol. 44, No. 7, pp. 1041-1048, 1996.
- [15] M. H. Al Sharkawy, A. Z. Elsherbeni, S. F. Mahmoud, "Electromagnetic scattering from parallel chiral cylinders of circular cross-sections using an iterative procedure," *Progress In Electromagnetics Research*, Vol. 47, pp. 87-110, 2004.
- [16] N. Engheta, and D.L. Jaggard, "Electromagnetic chirality and its applications," *IEEE Antennas and Propagation Society Newsletter*, Vol. 30, No. 5, pp. 6-12, 1988.
- [17] R. Ruppini, "Scattering of electromagnetic radiation by a perfect electromagnetic conductor cylinder," *J. Electromagn. Waves Appl.*, Vol. 20, pp. 1873-1880, 2006.
- [18] I. V. Lindell, and A. H. Sihvola, "Perfect electromagnetic conductor," *J. Electromagn. Waves Appl.*, Vol. 19, No. 7, pp. 861-869, 2005.

- [19] I.V.Lindell and A. H. Sihvola, "Realization of the PEMC boundary," *IEEE Trans. Antennas Propag*, Vol. 53, 3012-3018, 2005.
- [20] N. Montaseri, M. Soleimani, and A. Abdolali, "Realization of the perfect electromagnetic conductor circular cylinder using anisotropic media," *Progress In Electromagnetics Research*, Vol. 25, 173–184, 2012.
- [21] A. Shahvarpour, T. Koderä, A. Parsa and C. Caloz, "Arbitrary electromagnetic conductor boundaries using Faraday rotation in a grounded ferrite slab," *IEEE Trans. Microw. Theory Tech*, Vol.58, 2781-2793, 2010.
- [22] C. Caloz, A. Shahvarpour, D.L. Sounas, T. Koderä, B. Gurlek and N. Chama-nara, "Practical realization of perfect electromagnetic conductor (PEMC) bound-aries using ferrites, magnet-less non reciprocal metamaterials (MNMs) and graphene, in Proceedings of 2013 URSI," *International Symposium on Elec-tromagnetic Theory (EMTS)*, 652- 655, 2013.
- [23] P. M. Platzman and H. T. Ozaki, "Scattering of electromagnetic waves from an infinitely long magnetized cylindrical plasma," *J. of Appl. Phys.*, vol. 31, pp. 1597-1601; September, 1960.
- [24] C. XI. de Ridder and L. G. Peterson, "Scattering from a homogeneous plasma cylinder of infinite length," *M.I.T. Lincoln Laboratory, Lexington, Mass.*, Rept. No. 3126-4, 1962.
- [25] Y. L. Geng , X. B. Wu , and L. W. Li, "Analysis of electromagnetic scattering by a plasma anisotropic sphere," *Radio Sci.* Vol. 38, pp. 1-12, 2003.
- [26] J. R. David, and C. Melville, *Plasmas and controlled fusion*, New York, NY, USA: John Wiley & Sons; 1961.
- [27] L. Zeng, R. Song, X. Jian, "Scattering of electromagnetic radiation by a time reversal perturbation topological insulator circular cylinder ," *Modren Physics Letters B* , Vol. 27, No.14, pp. 1350098, 2013.

- [28] J.E. Moore, "Topological insulators: the next generation," *Nat. Phys.*, Vol. 5, pp. 378-380., 2009.
- [29] M.Z. Hasan, C.L. Kane, "Topological insulators," *Rev. Mod. Phys.*, Vol. 82, pp. 3045-3067, 2010.
- [30] X.L. Qi, T.L. Hughes, S.C. Zhang, "Topological field theory of time-reversal invariant insulators," *Phys. Rev. B*, Vol. 78, pp. 195424., 2008.
- [31] C.L. Kane, E.J. Mele, "Z₂ topological order and the quantum spin Hall effect," *Phys. Rev. Lett.*, 95, 146802, 2005.
- [32] X.L. Qi, T.L. Hughes, S.C. Zhang, "Topological field theory of time-reversal invariant insulators," *Phys. Rev. B*, Vol. 78, pp. 195424., 2008.
- [33] F. Liu, J. Xu, and Y. Yang, "Polarization conversion of reflected electromagnetic wave from topological insulator," *J. Opt. Soc. Am. B*, Vol. 31, No. 4, pp. 735-741, April 2014.
- [34] X.-L. Qi, R. Li, J. Zang and S. C. Zhang, "Inducing a magnetic monopole with topological surface states," *Science* Vol. 323, pp. 1184-1187, 2009.
- [35] Z. Shen, and C. Li, "Electromagnetic scattering by a conducting cylinder coated with metamaterials," *Progress In Electromagnetics Research*, PIER 42, 91-105, 2003.
- [36] E. Irci, and V. B. Ertürk, "Achieving transparency and maximizing scattering with metamaterial-coated conducting cylinders," *Phys. Rev. E*, Volume 76, 056603, 1-15, 2007.
- [37] F. R. Cooray, and Abdul-Kadir Hamid, "Scattering from a coated perfect electromagnetic conducting elliptic cylinder," *International Journal of Electronics and Communications*, Vol. 66, No. 4, pp. 472-479, 2012.

- [38] S. Ahmed, F. Manan, A. Shahzad, and Q. A. Naqvi, "Electromagnetic scattering from a chiral coated PEMC cylinder," *Progress In Electromagnetics Research M*, Vol. 19, 239-250, 2011.
- [39] W. G. Swarner, "Radar cross sections of dielectric or plasma coated conducting spheres and circular cylinders ," *IEEE Trans. Antennas Propagat.* Vol. 11, pp. 558-69, 1963.
- [40] H. C. Chen, and D. K. Cheng, "Scattering of electromagnetic waves by an anisotropic plasma-coated conducting cylinder," *IEEE Trans. Antennas Propagat.* Vol. 12, pp. 348-353, 1964.
- [41] A. Ghaffar, M. Z. Yaqoob, Majeed A. S. Alkanhal, M. Sharif, and Q. A. Naqvi, "Electromagnetic scattering from anisotropic plasma-coated perfect electromagnetic conductor cylinders," *Int. J. Electron. Commun. (AEU)*, Vol. 68, pp. 767-772, 2014.
- [42] A. Ghaffar et al, "Echo width of plasma coated topological insulator cylinder," *International Journal of Applied Electromagnetics and Mechanics*, Vol. 54, 489-499, 2017.
- [43] H. Y. She, L. -W. Li, Olivier J.F. Martin and J. R. Mosig, "Surface polaritons of small coated cylinders illuminated by normal incident TM and TE plane waves," *Optics Express*, Vol. 16, No. 2, pp. 1007-1019, 2008.
- [44] L. Ge, D. Han and Y. Wu, "Manipulation of plasmonic resonances in graphene coated dielectric cylinders ," *Progress in Electromagnetic Research Symposium (PIERS)*, pp. 2990-2990, 2016.
- [45] A. Q. Howard, "The electromagnetic fields of a subterranean cylindrical inhomogeneity excited by a line source," *Geophys.*, Vol. 37, pp. 975-984, 1972.
- [46] B. P. D'Yakonov, "The diffraction of electromagnetic waves by a circular cylinder in a homogeneous half-space," *Bull. Acad. U.S.S.R.*, pp. 950-955, 1959.

- [47] S. O. Ogunade, "Electromagnetic response of an embedded cylinder for line current excitation," *Geophys.*, Vol. 46, pp. 45-52, 1981.
- [48] S. F. Mahmoud, S. M. Ali, and J. R. Wait, "Electromagnetic scattering from a buried cylindrical inhomogeneity inside a lossy earth," *Radio Sci.*, Vol. 16, No. 6, pp. 1285-1298, 1981.
- [49] N. V. Budko and P. M. van den Berg, "Characterization of a two-dimensional subsurface object with an effective scattering model," *IEEE Trans. Geosci. Remote Sensing*, Vol. 37, pp. 2585-2896, 1999.
- [50] K. Hongo and A. Hamamura, "Asymptotic solutions for the scattered field of plane wave by a cylindrical obstacle buried in a dielectric half-space," *IEEE Trans. Antennas Propag*, Vol. 34, pp. 1306-1312, 1986 .
- [51] Q. A. Naqvi, A. A. Rizvi, and Z. Yaqoob, "Corrections to asymptotic solutions for the scattered fields of plane wave by a cylindrical obstacle buried in a dielectric half-space," *IEEE Trans. Antennas Propag*, Vol. 48, No. 5, pp. 846-849, 2000.
- [52] M. Di Vico, F. Frezza, L. Pajewski, and G. Schettini, "Scattering by a finite set of perfectly conducting cylinders buried in a dielectric half-space: a spectral-domain solution," *IEEE Trans. Antennas Propag*, Vol. 53, No. 2, pp. 719-727, 2005.
- [53] M. Di Vico, F. Frezza, L. Pajewski, and G. Schettini, "Scattering by buried dielectric cylindrical structures," *Radio Sci. RS6S18*, Vol. 40, 2005.
- [54] M. Akhtar, Nazir A. Naz, M.A. Fiaz and Q.A. Naqvi, "Scattering from topological insulator circular cylinder buried in a semi-infinite medium," *J. modern optics*, Vol. 61, No. 9. pp. 697-702, 2014.
- [55] S. Ahmed and Q. A. Naqvi, "Electromagnetic scattering from a perfect electromagnetic conductor cylinder buried in a dielectric half-space," *Progress in Electromagnetic Research*, Vol. 78, pp. 25-38, 2008.

- [56] D. E. Lawrence and K. Sarabandi, "Electromagnetic scattering from a dielectric cylinder buried beneath a slightly rough surface," *IEEE Trans. Antennas Propag*, Vol. 50, No. 10, pp. 1368-1376, 2002.
- [57] M. A. Fiaz, L. Pajewski, C. Ponti, G. Schettini and F. Frezza, "Scattering by a circular cylinder buried under a slightly rough surface: the Cylindrical-Wave Approach," *IEEE Trans. Antennas Propagat*, Vol. 60, No. 6, pp. 2834-2842, 2012.
- [58] L. Tsang, J. A. Kong, K. H Ding, and C. O. Ao, *Scattering of Electromagnetic Waves: Numerical Simulations*, New York (NY):, John Wiley & Sons Inc., 2001.
- [59] M. F. Chen, A. K. Fung, and J. R. Wait, "A numerical study of the regions of validity of the Kirchhoff and small-perturbation rough surface scattering models," *Radio Sci.*, Vol. 23, No. 2, pp. 163-170, 1988.
- [60] E. Thorsos, "The validity of the Kirchhoff approximation for rough surface scattering using a Gaussian roughness spectrum," *J. Acoust. Soc. Am.*, Vol. 83(1), pp. 78-92, 1988.
- [61] Y. Altuncu, A. Yapar, and I. Akduman, "On the scattering of electromagnetic waves by bodies buried in a half-space with locally rough interface," *IEEE Trans. Geosci. Remote Sensing*, Vol. 44, No. 6, pp. 1435-1443, 2006.
- [62] C. H. Kuo and M. Moghaddam, "Electromagnetic scattering from a buried cylinder in layered media with rough interfaces," *IEEE Trans. Antennas Propag*, Vol. 54, pp. 2392-2401, 2006.
- [63] M. A. Fiaz, C. Ponti, G. Schettini and F. Frezza, "Electromagnetic scattering by a circular cylinder buried below a slightly rough Gaussian surface," *J. Opt. Soc. Am. A* , Vol. 31, No. 1, pp. 26-34, 2014.

- [64] S. Iqbal, M. A. Fiaz, and M. A. Ashraf, "Scattering from a DNG coated PEMC cylinder buried beneath a sinusoidal/flat surface," *Int. J. Electron. Commun. (AEU)*, Vol. 70, pp. 58-63, 2016.
- [65] M. Kamran, M. A. Fiaz, and M. A. Ashraf, "Use of chiral coating to reduce RCS of PEC cylinder buried beneath a sinusoidal surface," *Int. Optik*, Vol. 127, pp. 1546-1552, 2016.
- [66] M. A. Fiaz, "Investigating the reduction of cross-polarized Gaussian beam scattering from a PEMC buried cylinder coated with a topological insulator," *Applied Optics.*, Vol. 57, No. 27, 2018.
- [67] A. Z. Elsherbeni, "A comparative study of two-dimensional multiple scattering techniques," *Radio Sci*, Vol. 29, pp. 1023-1033, Jul.-Aug. 1994.
- [68] Asghar, M., M. N. S. Qureshi, M. Akhtar, M. A. Fiaz, and M. A. Ashraf, "Scattering from anisotropic plasma-coated PEMC cylinder buried beneath a slightly rough surface," *Journal of Modern Optics*, Vol. 64, no. 2, pp. 101-110, 2017.
- [69] M. Akhtar, Arshad Fiaz, M., Aqueel Ashraf, M., "Gaussian beam scattering from a DNG chiral coated PEMC cylinder buried below slightly rough surface," *Journal of Electromagnetic Waves and Applications*, Vol. 31(9), 912-926, 2017.
- [70] M. Akhtar, M. A. Fiaz, and M. A. Ashraf, "On using the complex conjugate material as coating to observe scattering from a PEMC cylinder buried below a sinusoidal slightly rough surface," *Optik*, Vol. 225, 165570, 2021.
- [71] L.B. Felsen and N. Marcuvitz, *Radiation and scattering of waves*, Wiley-IEEE Press, 2001.

Turnitin Originality Report

On using the coating of different materials to reduce the cross polarized scattering from a PEMC cylinder buried below a rough surface by M. Akhtar

From DRSM (DRSM L)

- Processed on 06-Aug-2021 15:36 PKT
- ID: 1628394111
- Word Count: 7830

Similarity Index
10%

Similarity by Source

Internet Sources

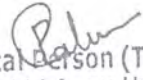
0%

Publications

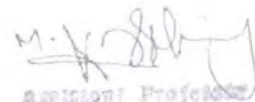
2%

Student Papers

4%


Focal Person (Turnitin)
Quaid-i-Azam University
Islamabad

Advisor
M. Ashad Fiaz


Assistant Professor
Department of Electronics
Quaid-i-Azam University
Islamabad

Sources:

1 3% match (student papers from 18-Aug-2015)
Submitted to Higher Education Commission Pakistan on 2015-08-18

2 1% match (student papers from 04-Nov-2016)
Submitted to Higher Education Commission Pakistan on 2016-11-04

3 1% match (publications)
Murtaza Ali, Ashad Fiaz, "Investigating the reduction of cross-polarized scattering from a PEMC buried cylinder coated with a topological insulator", Applied Optics, 2016

4 1% match (publications)
Murtaza Ali, Ashad Fiaz, "Scattering from a DNG coated PEMC cylinder with a rough surface", AEU International Journal of Electronics and Communications, 2016

5 1% match (publications)
Murtaza Ali, Ashad Fiaz, "Scattering from a dielectric coated PEMC cylinder with a rough surface", AEU International Journal of Electronics and Communications, 2016

6 < 1% match (student papers from 06-Aug-2015)
Submitted to Higher Education Commission Pakistan on 2015-08-06

7 < 1% match (student papers from 03-Jul-2015)
Submitted to Higher Education Commission Pakistan on 2015-07-03

Co Advisor:


M. Haseeb Ashraf
Assistant Professor
Department of Electronics
Quaid-i-Azam University
Islamabad


Chairman
Department of Electronics
Quaid-i-Azam University
Islamabad